Ponz-Segrelles, G.; Glasby, C.; Helm, C.; Beckers, P.; Hammel, J.; Ribeiro, R.; Aguado, M.:

Integrative anatomical study of the branched annelid Ramisyllis multicaudata (Annelida, Syllidae).

In: Journal of Morphology. Vol. 282 (2021) 6, 900 - 916.

First published online by Wiley: 04.04.2021

https://dx.doi.org/10.1002/jmor.21356

Integrative anatomical study of the branched annelid *Ramisyllis multicaudata* (Annelida, Syllidae)

Running title: Anatomy of *Ramisyllis multicaudata*

***Guillermo Ponz-Segrelles[a], Christopher J. Glasby[b], Conrad Helm[c], Patrick Beckers[d], Jörg U. Hammel[e], Rannyele Passos Ribeiro[a], and *M. Teresa Aguado[c]**

[a]Departamento de Biología, Facultad de Ciencias, Universidad Autónoma de Madrid, 28049, Madrid, Spain; [b]Museum and Art Gallery of the Northern Territory, PO Box 4646, Darwin, NT 0801, Australia; [c]Animal Evolution & Biodiversity, Georg-August-Universität Göttingen, 37073 Göttingen, Germany; [d]Institute of Evolutionary Biology and Ecology, University of Bonn, 53121 Bonn, Germany; [e]Institute of Materials Research, Helmholtz-Zentrum Geesthacht, Max-Planck-Straße 1, D-21502, Geesthacht, Germany

Corresponding authors:

*Guillermo Ponz Segrelles: Departamento de Biología, Facultad de Ciencias, Universidad Autónoma de Madrid, 28049, Madrid, Spain. Tel: +34689402289. E-mail address: guillermo.ponz.segrelles@gmail.com
*Maria Teresa Aguado: Animal Evolution & Biodiversity, Georg-August-Universität Göttingen, 37073 Göttingen, Germany. Tel: +49 (0)551 39-25536. E-mail address: aguadomolina@uni-goettingen.de

ORCID IDs:

Guillermo Ponz Segrelles: 0000-0003-3591-9052
Christopher J. Glasby: 0000-0002-9464-1938
Conrad Helm: 0000-0002-0308-8402
Patrick Beckers: 0000-0003-4051-9774
Jörg U. Hammel: 0000-0002-6744-6811
Rannyele Passos Ribeiro: 0000-0002-0304-7053
Maria Teresa Aguado: 0000-0002-5583-7516

Abstract

The sponge-dwelling Syllidae *Ramisyllis multicaudata* and *Syllis ramosa* are the only annelid species for which a branched body with one head and multiple posterior ends is known. In these species, the head is located deep within the sponge, and the branches extend through the canal system of their host. The morphology of these creatures has captivated annelid biologists since they were first discovered in the late XIXth century, and their external characteristics have been well documented. However, how their branched bodies fit within

their symbiotic host sponges and how branches translate into internal anatomy has not been documented before. These features are crucially relevant for understanding the body of these animals and, therefore, the aim of this study was to investigate these aspects. In order to assess these questions, live observation, as wells as histology, immunohistochemistry, micro-computed tomography, and transmission electron microscopy techniques were used on specimens of *R. multicaudata*. By using these techniques, we show that the complex body of *R. multicaudata* specimens extends greatly through the canal system of their host sponges. We demonstrate that iterative external bifurcation of the body is accompanied by the bifurcation of the longitudinal organ systems that are characteristic of annelids. Additionally, we also highlight that the bifurcation process leaves an unmistakable fingerprint in the form of newly-described "muscles bridges". These structures theoretically allow one to distinguish original and derived branches at each bifurcation. Last, we characterize some of the internal anatomical features of the stolons (reproductive units) of *R. multicaudata*, particularly their nervous system. Here, we provide the first study of the internal anatomy of a branched annelid. This information is not only crucial to deepen our understanding of these animals and their biology, but it will also be key to inform future studies that try to explain how this morphology evolved.

Keywords

Bifurcation; Annelida; Morphology; Stolon; 3D reconstruction

Research highlights

The internal anatomy of *Ramisyllis multicaudata* reflects the external bifurcated pattern. Within each branch, they are like other Syllidae. The branches are not lateral outgrowths but whole bifurcations involving all organs that have muscle bridges.

1. Introduction

Annelids are a group of animals that typically show a long, slender, segmented body (Rouse & Pleijel, 2001). Internally, they have a nervous system composed of a dorsal brain and a longitudinal ventral nerve cord joined by paired circumesophageal connectives. The digestive tract opens anteriorly in a sub-terminal mouth and posteriorly in a terminal anus. Furthermore, the circulatory system consists of two main longitudinal vessels, one dorsal and one ventral. Finally, the muscular system is usually composed of several pairs of dorsal and ventral longitudinal muscle bands combined, in most cases, with circular musculature (Bleidorn et al., 2015; Filippova et al., 2010; Helm et al., 2018; M. C. M. Müller, 2006; Orrhage & Müller, 2005; Purschke & Müller, 2006; Rouse & Pleijel, 2001; Tzetlin & Filippova, 2005).

In Syllidae, morphology and anatomy have been the subject of research since the XIXth century (e.g. Audouin & Milne Edwards, 1833; Grube, 1840). The classic anatomical studies of syllids are best represented by the comprehensive work of Alphonse Malaquin, whose observations laid the foundations of most of our current knowledge on this subject (Malaquin, 1893). In these early works, the general anatomy of syllids was described and they were found to have a strongly regionalized digestive tract with an anterior, partially-eversible foregut. Additionally, a prominent ventral nerve cord with a variable number of connectives and neurite bundles; dorsal and ventral median blood vessels; and a muscle system with strongly developed longitudinal muscles and comparatively reduced circular ones are present in most taxa (Malaquin, 1893). Within this general anatomical framework, the most noteworthy and distinctive anatomical feature of syllids is the proventricle. The proventricle is the region of the digestive tract that lies immediately posterior to the more strongly-cuticularized, partially-eversible axial pharynx, and is characterized by a prominent layer of radially-arranged muscle cells (Haswell, 1921; Malaquin, 1893; Pleijel, 2001; San Martín, 2003; San Martín & Aguado, 2014).

Interestingly, although these early studies already revealed much of the general architecture of the syllid body, most of the work that has been done in the family is either taxonomical, or systematic. Consequently, because most taxonomic characters within Syllidae are either external, or can be seen by transparency by using light microscopy (Aguado et al., 2012; San Martín, 2003; San Martín & Aguado, 2012, 2014), internal anatomy has not been a traditional focus of syllid research, as indicated by Parapar, Caramelo, Candás, Cunha-Veira, & Moreira (2019). However, in recent years several studies have started using combinations of different morphological techniques that allow for a better, more detailed understanding of the anatomical features of these annelids. These combined approaches include the usage of traditional techniques such as histology or electron microscopy, with others such as immunohistochemistry and confocal Laser Scanning Microscopy (cLSM; Aguado, Helm, et al., 2015; Helm & Capa, 2015; Schmidbaur et al., 2020; Weidhase et al., 2016, 2017), or micro-computed X-ray tomography (µCT; Faulwetter et al., 2013; Parapar et al., 2017, 2019).

Nevertheless, Syllidae is a species-rich family with more than one thousand described species (Martin et al., 2021; Pamungkas et al., 2019). Therefore, within-family anatomical variation is to be expected. One example of this within-family variability has been recently revealed by the extraordinarily detailed investigation of the nervous system of 21 species from all subfamilies (Schmidbaur et al., 2020).

Remarkably, among the wide range of forms that exist in Syllidae, two species stand out, namely *Syllis ramosa* McIntosh, 1879 and *Ramisyllis multicaudata* Glasby, Schroeder, & Aguado, 2012. These two species are unique in that their bodies consist of an otherwise normal syllid anterior end, which is followed by an enormous branching body in which some segments show lateral bifurcations (Glasby et al., 2012; McIntosh, 1879, 1885; Oka, 1895; Okada, 1937). *S. ramosa* and *R. multicaudata* are species whose individuals live symbiotically confined within the canal system of respective specific sponge species (Glasby et al., 2012;

Izuka, 1912; Oka, 1895; Okada, 1937). Interestingly, although they start their lives as bilateral annelids, they later develop lateral branches that themselves recursively produce new lateral branches, thus creating an asymmetric pattern (Glasby et al., 2012; McIntosh, 1879, 1885; Figure 1). Externally, adults of both species are characterized by a dendriform body; a more or less circular cross-section; an alternating size pattern of the dorsal cirri most pronounced in the mid- and posterior body; and the presence of a single type of simple, tomahawk-shaped chaetae (Glasby et al., 2012; McIntosh, 1879, 1885). Like many other syllids, the reproduction of *S. ramosa* and *R. multicaudata* is mediated by intermediate forms called stolons (Glasby et al., 2012; McIntosh, 1879, 1885; Okada, 1937; Read, 2001; Schroeder et al., 2017). Stolons are independent reproductive units that are formed at the posterior end of the body. These units are characterized by a variable number of segments that develop gonads and gametes, specially-shaped swimming chaetae, and a simple head with its own eyes. Once a stolon is ready it detaches from the rest of the body and swims freely until it mates and dies (Franke, 1999). In particular, stolon production in *R. multicaudata* has been shown to be of the gemmiparous type, i.e., several stolons are produced at the same time and from newly formed segments instead of being the result of metamorphosis (Glasby et al., 2012; Schroeder et al., 2017). Notably, this type of stolon development is common in the so-called “ribbon clade” to which the genus *Ramisyllis* belongs (Aguado, Glasby, et al., 2015; Álvarez-Campos et al., 2018). Furthermore, it has been proposed that gemmiparity might be related with the evolutionary origin of the branched body of these animals (Aguado, Glasby, et al., 2015).

As explained above, the external features of these species are reasonably well known and there are some known details about their reproduction, particularly in the case of the more recently studied *R*. *multicaudata*. However, how their distinctive morphology relates to internal anatomy has never been studied besides observing that the whole body has an interconnected digestive tract with a high number of ani, one per each posterior end (Glasby et al., 2012; McIntosh, 1879). Thus, many basic and relevant anatomical and functional

questions related to the branched bodies of these species remain to be answered, for example, the organization of internal structures as the ventral nerve cord, the blood vessels, or the longitudinal muscles. It is still unknown whether these structures simply ramify at the branching points and develop within morphologically and functionally similar branches, or whether there is an internal reorganization involving rearrangements in the presence, location, or number of structures at different body locations. Moreover, the branch distribution and ability of these animals to move within their host remain unclear.

Here, we present an integrated anatomical study of *R. multicaudata* in which we combine histology, transmission electron microscopy (TEM), cLSM, and µCT techniques. Based on these data, we provide a three-dimensional reconstruction of how these animals arrange themselves within their host sponges and describe their internal anatomy for the first time. In particular, we focus on the anatomy of the segments at which the body divides. Additionally, the anatomy of the musculature shows that it would be theoretically possible to follow the original (embryonic) anteroposterior axis from the head to the first-developed posterior end. We also describe internal anatomical details of the stolon's muscular and nervous systems. Finally, we discuss possible functional implications that derive from having a dendriform body.

2. Materials and Methods

2.1. Sampling, captivity, and dissection

Sponges of the genus *Petrosia* were collected from the type locality of *Ramisyllis multicaudata* Glasby, Schroeder & Aguado, 2012 adjacent to Channel Island Bridge in Darwin Harbour (12°33'17"S 130°52'27"E; Northern Territory, Australia). Sampling took place during the spring tides of December 2014, November and December 2017, and July 2018. Collection was done by hand while reef walking, as previously described (Glasby et al., 2012). After collection, the sponges were kept in a 75 L tank filled with natural seawater at the Museum and Art Gallery of

the Northern Territory (MAGNT). The tank was equipped with a filtering pump (HETO QD-1900), a protein skimmer (Aquatopia Marine Protein Skimmer & Filter 500 L/h), and a 10 h/14 h day/night light cycle using two florescent tubes (18000 K and 5000 K). To maintain the best possible conditions in the tank, daily 50% water changes were made with freshly collected clean natural sea water. Exposure of the sponges to air was avoided in order to minimize stress and tissue necrosis due to air bubbles being trapped in the canal system. Both the sponges and the worms survived in this aquarium system for up to 21 days while they were being processed and fixed for further analyses.

After collection, careful dissection of each sponge was carried out following the strategy described by Glasby et al. (2012). The obtained pieces of *R*. *multicaudata* were preserved and treated as described under each technique's subheading. Additionally, two entire undissected sponges were preserved in 100% ethanol and deposited as a reference at MAGNT (NTM Z007518) and at the Biodiversity Museum in Göttingen (ZMUG 29420). Last, the obtained histological sections as well as the dissected specimens of *R. multicaudata* were deposited at the Biodiversity Museum in Göttingen (ZMUG 29421 and 29422, respectively).

2.2. Synchrotron radiation micro-computed tomography

Two complete, undissected sponges were preserved in a 6:3:1 mixture of 80% ethanol, 35% formaldehyde and 100% acetic acid for 24 hours. During this process, the fixative was stirred multiple times to ensure adequate fixation. After that, samples were dehydrated in ascending ethanol series before long-term storage in 100% ethanol. Following fixation, fragments of the sponges were trimmed off until adequately sized pieces were obtained (see sizes below).

Once trimmed, the first specimen was stained in 1% iodine solution and critical point dried. Synchrotron radiation-based micro-computed tomography scans of this critical point dried sponge were recorded at the Imaging Beamline P05 (IBL; Greving et al., 2014; Haibel et al., 2010; Wilde et al., 2016) operated by the Helmholtz-Zentrum-Geesthacht at the storage ring

PETRA III (Deutsches Elektronen Synchrotron – DESY, Hamburg, Germany). Imaging was done at photon energy of 35 keV. Projections were recorded with a sample to detector distance of 200 mm using a custom developed 20 MP CMOS camera system (Lytaev et al., 2014) with an effective pixel size of 1.28 µm. For each tomographic scan 3601 projections at equal intervals between 0 and π were recorded. Tomographic reconstruction was done by applying an intensity phase retrieval transport and using the filtered back projection algorithm (FBP) implemented in a custom reconstruction pipeline (Moosmann et al., 2014) using Matlab (Math-Works) and the Astra Toolbox (Aarle et al., 2015, 2016; Palenstijn et al., 2011). In order to enlarge the available field of view, the recorded projections were stitched prior to the tomographic reconstruction. After stitching, the projections were binned four times for further processing resulting in a reconstructed volume with an effective voxel size of 5.1 µm. Horizontal and vertical stitching of the recorded projections was necessary since the sample was much larger (≈1 cm^3) than the available field of view. The stitched projection covering the entire investigated specimen resulted in a field of view of 18.8 x 16.8 mm^2. For visualization and further analysis of the *R. multicaudata* specimen, the tomographic data was filtered by applying a mask in order to discriminate between sponge and annelid tissue. The mask was created by manual segmentation in Amira 6.7 (Thermo Fisher Scientific). VG Studio Max (Volume Graphics) was used for three-dimensional volume rendering.

The sponge piece created from the second preserved specimen was too large (≈11.5 cm^3) to be scanned as explained above and was imaged using a benchtop x-ray system (Nanotom S, PHOENIX X-ray). For that, the specimen was stained in 1% iodine solution and imaged in 70% EtOH. 2400 equally spaced projections between 0 an 2π were recorded. An acceleration voltage of 60 kV and a current of 170 µA was used. Tomographic reconstruction was done using the manufacturer's supplied software tool. The effective voxel size in the tomographic reconstructed volume was 14.2 µm. Data analysis was done following the above-mentioned workflow.

2.3. Histology and 3D reconstruction

For Azan staining, fragments of *R. multicaudata* were anesthetized in 7% $MgCl_2$ hexahydrate (mixed with seawater 1:1) and fixed for 24h in Bouin's solution (saturated aqueous picric acid, 37% formaldehyde, glacial acetic acid; 15:5:1 by volume). Then, the fixed samples were washed several times in ascending ethanol series before long-term storage in 70% ethanol. Afterwards, specimens were treated, stained, and sectioned following existing protocols (Beckers et al., 2013). Subsequent digital sectioning and 3D reconstruction was performed with the TrakEM2 plugin of Fiji 1.51v9 (Cardona et al., 2012; Schindelin et al., 2012). Blender 2.79b https://www.blender.org/ was used to render the final images of the histological 3D model.

2.4. Transmission electron microscopy (TEM)

Fragments of the middle and posterior body for TEM were anesthetized in 7% $MgCl_2$ hexahydrate (mixed with seawater 1:1) and fixed in 2.5% glutaraldehyde/1x PBS (phosphate buffered saline pH 7.4) for 1.5h while shaking at room temperature. Afterwards, the fixative was removed and the samples were washed three times in 1x PBS for 45 minutes each at room temperature. Once washed, the samples were preserved in 1x PBS containing 0.05% sodium azide at 4°C. After fixation, the specimens were postfixed in 1% OsO4 buffered in 0.05 $mol \cdot l^{-1}$ phosphate 0.3 $mol \cdot l^{-1}$ saline at 4°C for 1 h, subsequently dehydrated in an ascending acetone series followed by propylene oxide and embedded in Araldite. Ultra-thin sections of 70 nm thickness were cut on a LEICA UC6 ultramicrotome, placed on formvar coated, copper single slot grids (1 x 2mm) and automatically stained with uranyl acetate and lead citrate (QG-3100, Boeckler Instruments). After preparation, the sections were analyzed with a ZEISS EM10CR transmission electron microscope and documented on phosphor imaging plates (DITABIS).

2.5. Immunohistochemistry and confocal laser scanning microscopy (cLSM)

Pieces of the animal were anesthetized in $MgCl_2$ hexahydrate (7% stock solution in distilled water), and then fixed in 4% paraformaldehyde in PTW (phosphate buffered saline pH 7.4 +

0.1% Tween 20) for 2.5h while shaking at room temperature. Afterwards, samples were washed several times in PTW before long-term storage at 4°C in PTW + 0.05% Sodium azide. After fixation, immunohistochemical stainings were performed according to existing protocols (Helm et al., 2018; Weidhase et al., 2014). Accordingly, the proteinase K treatment was set to 10-15 min. For nervous system stainings, antibodies against acetylated α-Tubulin and Serotonin were used (see Helm et al., 2018 for details). Staining of musculature was performed with the f-actin marker Phalloidin-Rhodamine (see Weidhase et al., 2014 for details). Nuclear staining was performed with DAPI. Samples were scanned with a Leica SP8 cLSM. Image stacks were processed using Imaris 9.3 (Bitplane) and images were edited using Photoshop CC (Adobe).

3. Results

3.1. Observations from living specimens

The specimens of *Ramisyllis multicaudata* used for this investigation were all adults and showed the usual external features of the species [i.e., a dendriform body shape that develops post-embryonically (Figure 2); tomahawk-shaped chaeta; dorsal cirri with a strong, alternating pattern in their size, colour, and orientation; and a cream-coloured proventricle]. The animals were observed to be highly mobile within the sponges, the posterior ends being very active and occasionally extending outside of the sponge and crawling on its surface (Figure 1B; Supplementary online material, Video 1). Moreover, they were able to abandon parts of the sponge when disturbed or exposed to air for some time. In one case, a sponge was rapidly decaying and numerous posterior branches of the worm could leave the canal system; however, the whole specimen was not able to abandon the sponge.

Upon dissection of the sponges, we observed that the posterior and middle regions of the body of the *R. multicaudata* specimens were extremely elastic. Hence, the segments were able

to stretch until they had reached three or four times their original length. The anterior portion of the specimens was often located in the basal part of the sponge; it was never observed to be close to the surface of the sponge. Additionally, the anterior region was always considerably less active than the posterior ends.

Once extracted from the sponges, the animals always presented a bright white substance in the glands of the large dorsal cirri of the mid and posterior body. Additionally, pieces of the animal that were kept outside the sponge tissue for too long (one or two hours) quickly started to degenerate. This process was first hinted at by the content of the cirri glands often being expelled. Furthermore, a colour change of the latter was observable - from its usual white to an intense red both inside and outside the glands. No sponge tissue was visible within the gut of the worms. In fact, the intestine seemed to be always empty of any food particles along the entire length of the animals.

Detached stolons were sometimes present within the dissected sponges. When this happened, all of them were of the same sex and their sex always matched that of the stolons that were still attached to the worm's body. These free stolons usually had natatory chaetae and were able to swim, performing the strong oscillatory movement as observed in other syllid stolons. Although no experiment was performed, we observed that male stolons had a faster and more active swimming behaviour than female stolons, which were able to swim, but were prone to resting motionless at the bottom of the container.

3.2. Arrangement within the sponge

After preservation of undissected sponges, µCT-scans were used to generate three-dimensional models of two sponges with its inhabiting worms. This allowed for a better understanding of how *R. multicaudata* arranges itself within the canal system (Figure 3 Supplementary online material, Video 2 and Animated GIFs 1 and 2). These models confirmed the live observation that the animals branch to a high order without following any

recognizable pattern and widely occupy the sponge's canal system. Moreover, they also showed that while the internodes between branches are sometimes quite long, there are regions where branching occurs much more frequently. This form with one head and an intensively branched body that grows without a recognizable pattern generates a shape that has no plane of symmetry (despite each individual segment, as well as the array of segments between two branching points, being bilaterally symmetric).

3.3. General internal anatomy

Histological sections as well as TEM and cLSM were used to investigate the internal anatomy of *R*. *multicaudata* (Figures 4-6; Supplementary online material, Video 3). Histological examination of the internal anatomy of the anterior end (up to the first branching point) revealed that internal organs in *R*. *multicaudata* specimens are similar to those of other syllids. The animals have a thin outer cuticle produced by a simple cuboidal epithelium that is densely covered with microvilli (Figures 4; 5A, B). On the inside, they have a prominent coelomatic cavity, dorsal and ventral median blood vessels, a centrally located digestive tract, a basiepithelial ventral nerve cord, and musculature mainly composed of two dorsolateral and two ventral longitudinal muscle bands (Figure 4A–F). However, all longitudinal muscle bands are thin, sometimes even difficult to see (Figure 4C). Circular muscles are greatly reduced or completely absent and it was not possible to observe them with the methods used here. Additionally, within this general organization, it is worth noting that although the blood vessels, particularly the ventral one, are remarkably large, sometimes being even bigger than the intestine in diameter (Figure 4E), they are not associated with strong musculature at any point. Last, the segmental organs that have been often shown to be associated with the ventral base of the parapodia are also present, even in relatively anterior segments right after the ventricle (Figure 4D).

The animals show a long, slender, cylindrical, strongly-cuticularized pharynx formed by a simple columnar epithelium (Figure 4A). The pharynx has no tooth or trepan. Additionally, the paired structures that have often been called salivary or pharyngeal glands in other syllids can be distinguished (Figure 4A). Protractor and retractor muscles can also be seen in association with the pharynx. The proventricle is as wide as the whole body, completely filling the coelomic cavity to a point where it even squeezes the dorsal and ventral blood vessels (Figure 4B). The characteristic gigantic, radially-arranged muscular fibres are easily observable, and the gut lumen is reduced in diameter and surrounded by a densely packed simple columnar epithelium covered by a thin cuticle. Two lateral proventricular plates with a thicker cuticle where observed (Figure 4B). Posterior to the proventricle, the animals have a short ventricle without any caeca. The ventricle is characterized by a thick and complex epithelium covered by a thin cuticle and a laterally flattened lumen. From the current data, it cannot be clearly distinguished whether the ventricular epithelium is pseudostratified or truly stratified. Posterior to the ventricle, the digestive tract continues into the intestine. The intestine is notably small in diameter and it is cylindrical rather than moniliform, i.e., its diameter is more or less constant instead of showing a clear segmental increase and intersegmental decrease in diameter as is commonly found in many Syllidae. Because of this reduced diameter and its cylindrical shape, the intestine does not completely fill the coelomic space (Figure 4D-F). As for the intestinal epithelium, histological sections revealed that it is possible to distinguish between a more anterior part of the intestine where a thicker pseudostratified epithelium is present (Figure 4D), and a more posterior one where the epithelium becomes simple and much thinner, almost squamous (Figure 4F). Transmission electron microscopy and cLSM of the epithelium of the posteriormost part of the intestine (the rectal intestine close to the anal opening) documented that it is densely covered by microvilli and cilia (Figures 5C, D; 6A, B).

3.4. Internal anatomy at the branching point

As explained above, the main feature that distinguishes *R*. *multicaudata* from other annelids is the presence of a branched body. This morphology raises numerous questions about these animals, but perhaps the most basic one is how this external appearance relates to its internal anatomy. Thus, as part of this anatomical examination, we also used histological sections as well as cLSM to assess how internal organs are arranged at the animals' bifurcations. The histological sections were used to generate a three-dimensional model of the anterior end of one specimen, from the head to the first branching point (Figure 7; Supplementary online material, Animated GIF 3). All longitudinal internal structures branch at the bifurcations (Figures 4E; 7), and post-branch anatomy is completely comparable to that of the anterior end before the first branching point (Figures 4; 7; Supplementary online material, Video 3). Previously-unnoticed muscular 'bridges' cross over the intestine on the dorsal side and between the ventral nerve cord and the ventral blood vessel in the ventral side on one of the three paths coming out of the branching point (Figures 7B, C). The existence of these muscle bridges was also confirmed using immunohistochemical f-actin staining and subsequent confocal imaging on several branching points at different body positions of different individuals (Figures 8A, B).

In order to get further insight into the branching of the nerve cord, immunohistochemical stainings against acetylated-α-tubulin and serotonin were performed. Anti-α-tubulin antibodies predominantly stain the peripheral nerves and the ventral nerve cord, whereas the anti-serotonin antibody stains the cell bodies of regularly arranged serotonergic neurons within the ventral nerve cord. The stainings revealed that the emerging nervous system in derived branches has a structure similar to the previously existing ones, and that it does not replace any pre-existing nerve (Figures 8C, D).

3.5. Internal anatomy of stolons

The nervous and muscular system of the anterior end of attached and detached stolons was investigated by using immunohistochemical stainings and subsequent cLSM (Figure 6C, D). These stainings revealed that the stolons have a dorsal brain that is stained with both anti-acetylated-α-tubulin and anti-serotonin antibodies, and that they have a regular disposition of the ventral nerve cord and the segmental nerves. However, these stainings also documented special features about the stolon nervous system: (1) there is an intensively-stained ring of serotonergic cells located at the boundary between the stolon's head and the immediately anterior segment where the new pygidium is already developing ventrally (Figure 6C). (2) The density of nerve endings in the anterior margin of the stolon's head is high (Figure 6D). (3) The stolon's brain connects to the ventral nerve cord by a pair of circumintestinal connectives (Figure 6D).

Figure 6C shows that although the muscles of the developing stolon are continuous with those of the rest of the body, the muscle bands are greatly reduced in diameter when going through the narrow space by which the stolon is attached. Following this initial thin portion of the muscle bands in the stolon's head, the rest of the stolon's body possesses a well-developed longitudinal musculature in which the muscle bands are more prominent in size than those in the segments immediately anterior to the stolon (Figure 6C).

4. Discussion

Ramisyllis multicaudata and *Syllis ramosa* are the only annelid species for which a permanently and iteratively branched body is known (Glasby et al., 2012; Aguado, Glasby, Schroeder, Weigert, & Bleidorn, 2015). This morphology was first described in 1879 by William McIntosh when he wrote: "the body of the annelid [*Syllis ramosa*] appears to have a furor for budding" (McIntosh, 1879, p. 54). After McIntosh's original report, some further studies on the

morphology of *S. ramosa* were carried out during the late XIXth and early XXth centuries (Izuka, 1912; McIntosh, 1885; Oka, 1895; Okada, 1937). In these studies, despite some initial confusion regarding the presence or absence of one or multiple heads (McIntosh, 1879, 1885), *S. ramosa* was rapidly recognized as a single-headed syllid with a branched body. Furthermore, it was proposed that two types of branching occurred in *S. ramosa*: unilateral, and bilateral (Oka, 1895; Okada, 1937; see Glasby et al., 2012 for differences with *R. multicaudata*). Interestingly, already in the earliest reports of this phenomenon, McIntosh described that all branches contained a portion of the digestive tract, and that each posterior end had its own anus (McIntosh, 1879). Upon this observation, McIntosh even wondered how an animal like this could work on the inside and said that "it would seem that […] the tail and the anus were more useful than the head" (McIntosh, 1879, p. 54). Unfortunately, however, neither of the authors studying *S. ramosa* went any further with the study of internal anatomy. Therefore, the data reported here on the anatomy of *R. multicaudata* can only be compared to what is known in unbranched syllids.

4.1. Epidermis, cuticle, and musculature

The epidermis of annelids is generally composed of a cellular monolayer covered with a cuticle (Gardiner, 1992; Hausen, 2005). Within this epidermal layer, there are cells that present microvilli that protrude outside the cuticle and are in direct contact with the outer environment (Hausen, 2005; Mill, 1978). In syllids, the ultrastructure of the cuticle and epidermis of *Syllis amica* Quatrefages, 1866 was studied by Boilly, who found it to be rich in microvilli (Boilly, 1967). More recently, at least two studies on syllid anatomy have been conducted, including a detailed study of the anatomy of *Syllis gracilis* Grube, 1840. These studies have revealed similarly arranged epithelia (Parapar et al., 2019; Weidhase et al., 2016). However, the authors of those studies did not include any ultrastructural investigation and it is, thus, not possible to assess the presence or absence of microvilli in the epidermis of these species. The results shown here for *R. multicaudata* indicate that the epidermis consists of a

cellular monolayer in which there is a high number of microvilli, something that is consistent to what has been previously shown for these other species.

As for the musculature, it has been repeatedly shown that many annelid groups (including several Phyllodocida) do not possess circular muscles. In these cases, their bracing function is carried out by the so-called bracing muscles that are associated with the parapodial muscle complex (Purschke & Müller, 2006; Tzetlin et al., 2002; Tzetlin & Filippova, 2005). In syllids, supralongitudinal transverse muscle fibers have been found in specimens of *Myrianida prolifera* (O. F. Müller, 1778) and *Typosyllis antoni* Aguado, Helm, et al., 2015 (Aguado, Helm, et al., 2015; Filippova et al., 2010). Regarding *R. multicaudata*, a reduction or loss of circular musculature would be consistent with the hypothesis proposed by Tzetlin & Filippova (2005), who argued that this type of musculature plays a greater role in borrowing species than in those with other modes of locomotion (which might be particularly true in the case of sponge-dwelling species). However, even though no circular musculature was observed in the specimens studied here, a more detailed investigation regarding the fine structure of the muscle system would be needed in order to completely rule out the presence of circularly-arranged muscle fibers in *R. multicaudata*.

In the case of longitudinal musculature, the dorsolateral and ventral longitudinal muscle bundles of *R. multicaudata* are small when compared with those of other syllid species like *T. antoni* and *S. gracilis* (Aguado, Helm, et al., 2015; Parapar et al., 2019; Weidhase et al., 2016). As in the case of circular musculature, this poorly developed longitudinal muscle system might be the result of the symbiotic lifestyle of this species. Additionally, it might also be related to the observed increased elasticity of *R. multicaudata* with respect to other syllid species.

4.2. Coelom, blood vessels and segmental organs

The internal anatomy of *R. multicaudata* is characterized by a wide coelomic cavity in which only a relatively small portion is occupied by the organs. According to Malaquin (1893), syllids

usually have moniliform digestive tracts in which the intestinal walls are pushed outwards by the gut's content and lie close to the coelomic peritoneum of the body wall. This disposition of the intestine that results in a narrow coelomic cavity can be seen by transparency in many syllids, and it has been clearly shown in the histological study of *T. antoni* (Weidhase et al., 2016). However, wide coelomic cavities with cylindrical rather than moniliform intestines similar to the one found in *R. multicaudata* have been previously reported for other syllids such as *Syllis garciai* (Campoy, 1982) and *S. gracilis* (Faulwetter et al., 2013; Parapar et al., 2017, 2019). Parapar et al. (2019) described incomplete septa in the foregut region of *S. gracilis*, which is required for the foregut to be able to move along the anteroposterior axis. This would also mean that the coelomic fluid can move among the segments freely, at least in the anterior region. The data provided here is not enough to distinguish whether the intersegmental septa are complete or not, but a condition similar to that of *S. gracilis* can be expected for all syllids since this is the only way in which the pharynx can be eversible.

Regarding the circulatory system, although all annelids have the same general arrangement of the main vessels, the specific disposition of smaller vessels within each segment can be variable (Gardiner, 1992). Within Syllidae, the presence of a dorsal and a ventral longitudinal blood vessel without heart bodies was already recognized by Malaquin (1893). However, he also recognized that the small size of syllids makes the study of their circulatory system difficult. Consequently, his description did not go any further than noting that the circulatory system was closed, and that the two main vessels were connected by circumesophageal connectives (Malaquin, 1893). More recently, different studies have shown that although the general architecture described by Malaquin is conserved across different species (Parapar et al., 2019; Weidhase et al., 2016), additional lateral longitudinal vessels can be found in *S. garciai* (Parapar et al., 2017). In the case of *R. multicaudata*, the data presented here shows that the general organization of its circulatory system is similar to what Malaquin described for other syllid species despite having a more complex body. Yet, it presents at least one

noteworthy feature, namely, the presence of enlarged blood vessels in the anterior body (see Figures 4; 5A; 7; Supplementary online material, Video 3). Assuming that blood circulation works in *R. multicaudata* in a way that is comparable to that of other annelids, all the body's blood needs to be carried anteriorly by the longitudinal dorsal vessel all the way to the circumesophageal ring. Afterwards, the blood is distributed back to the different branches by the longitudinal ventral vessels (Gardiner, 1992). If this assumption is correct, the vessels of the anterior region might need to be larger in order to accommodate the increased amount of blood that comes from the numerous posterior ends.

As for the segmental organs, these are likely comparable to the segmental organs that have been recently reported in *S. gracilis* (Parapar et al., 2019). Notably, these structures have been long recognized as part of the nephridial system of syllids (Bartolomaeus, 1999; Fage, 1906; Goodrich, 1900, 1945; Kuper, 2001; Malaquin, 1893). Similar to that described in these previous investigations, the segmental organs of *R. multicaudata* appear in a ventrolateral position close to the base of the parapodia.

4.3. Digestive tract

The digestive tract of syllids has been traditionally divided into two parts: a markedly regionalized foregut of ectodermic origin, and a much less differentiated intestine of endodermic origin (e.g. Malaquin, 1893; Parapar et al., 2019; San Martín & Aguado, 2014). The foregut has been studied in the past by several authors (Boilly, 1967; del Castillo et al., 1972; Delgado et al., 1992; Haswell, 1921; Malaquin, 1893; Michel, 1974; Parapar et al., 2019; San Martín & Aguado, 2014; Tzetlin & Purschke, 2005; Weidhase et al., 2016) and it has been shown that it is always of the axial muscular type (sensu Tzetlin & Purschke, 2005). This axial muscular foregut can be divided in at least three parts: a pharyngeal sheath that immediately follows the mouth opening; a long, strongly-cuticularized, partially-eversible pharynx; and a muscular proventricle that is thought to act as a suction pump for intake and outtake of water

and food. Additionally, the pharynx may or may not be furnished with a terminal trepan and/or a subterminal or posterior single dorsal tooth, as well as with a variable number of long anterior glands that protrude into the coelom and run posteriorly parallel to it. Furthermore, the proventricle may present a pair of lateral more strongly-cuticularized plates [e.g. *Syllis malaquini* (Ribeiro et al., 2020)]. As described above, the foregut of *R. multicaudata* has all three usual regions and the proventricle bears a pair of lateral plates. In adult specimens, there is no trepan or tooth (a tooth was observed in juveniles only; Glasby et al., 2012). Pharyngeal armature is present in almost all members of the ribbon clade, which usually have a trepan and sometimes also a dorsal tooth (Álvarez-Campos et al., 2013, 2018; Imajima & Hartman, 1964). The lack of all these structures in *R. multicaudata* could be related to the feeding habits present in this species (which are still unknown). However, the exact functioning of the foregut of syllids has not been fully described yet. Hence, it remains difficult to interpret the lack of these structures in functional terms.

Posterior to the proventricle, the ventricle was originally considered as a fourth part of the foregut (e.g. Malaquin, 1893). However, despite there being no information as for its germ layer origin, more recent accounts have considered it as part of the intestine (Tzetlin & Purschke, 2005). The results presented here show that the ventricular epithelium is covered by a thin cuticle, which might indicate that it is more likely of ectodermic origin. Either way, as it has been shown in the case of *R. multicaudata*, the ventricle is a variable but generally short portion of the digestive tract characterized by its thick, complex secretory epithelium (Haswell, 1921; Malaquin, 1893; Parapar et al., 2019; Weidhase et al., 2016). The ventricle might be reduced or absent in some species and, when present, it may give rise to two lateral caeca (Haswell, 1921; Malaquin, 1893). These caeca have been proposed to act as chambers in which pumped-in water is accumulated as part of the feeding process before being expelled trough the mouth again (Malaquin, 1893), but also as a sort of “swimming bladder” that regulates buoyancy (Jeuniaux, 1969). Nevertheless, although the first of these functions seems to be

more likely, the lack of detailed knowledge about the role these structures makes it difficult to interpret what their absence in *R. multicaudata* can reveal about the biology of this species.

The intestine completes the remaining part of the digestive tract extending from the posterior end of the ventricle to the short rectum immediately before the anal opening. The intestinal epithelium of annelids generally consists of a cell monolayer throughout its entire length. However, it can be divided into an anterior portion (with a thicker epithelium and abundant secretory cells) and a posterior portion (with a thinner epithelium and less secretory cells; Malaquin, 1893; Saulnier-Michel, 1992). In *R. multicaudata*, this distinction can be seen as a variation in the thickness of the epithelium along the intestine. However, there is no clear boundary between these two regions of the intestine. Again, despite there being some data about the diet of syllids (Giangrande et al., 2000; Jumars et al., 2015), the current knowledge about the physiology of digestion in syllids (or, indeed, annelids in general) is limited (see Jeuniaux, 1969; Mill, 1978), a fact that considerably limits any further interpretations of morphological data.

As mentioned, the general anatomy of the digestive tube of *R. multicaudata* is similar to that of other syllids. These similarities include the presence of strong ciliation in the posterior gut, a feature that is often associated with nutrient absorption (Malaquin, 1893; Saulnier-Michel, 1992) and that may indicate that the gut of these animals is, at least, partially functional. If this interpretation is correct, it would only deepen the mystery of how they manage to feed their enormous bodies through a regular-sized mouth and with a regular-sized foregut. Notably, this question was already asked by McIntosh (1879) when he first described *S. ramosa* and that could not be answered by previous works on *R. multicaudata* (Aguado, Glasby, et al., 2015; Glasby et al., 2012). As explained above, the epidermis of *R. multicaudata* shows long microvilli that protrude outside the cuticle and that could potentially be involved in obtaining of

nutrients from the surrounding water (Glasby et al., 2012). Future work is needed in order to assess functional questions such as this one.

4.4. Nervous system

The nervous system of different syllid species has been recently studied in detail by Schmidbaur et al. (2020). In their study, these authors show how syllids are notably variable in several aspects of their nervous system, such as the fine anatomy of the brain and the innervation patterns of anterior structures. However, the general architecture of the brain; the basiepithelial, trineuralian ventral nerve cord; the innervation of parapodia; and the basic structure of the stomatogastric nervous system are all fairly conserved within the family (Schmidbaur et al., 2020). Here, we show that the anterior end of *R. multicaudata* specimens has a nervous system similar to those that have already been described in Syllidae. This includes a dorsal brain and a basiepithelial ventral nerve cord connected by paired circumesophageal connectives, as well as four pairs of major segmental neurite bundles (Malaquin, 1893; Parapar et al., 2019; Schmidbaur et al., 2020; Weidhase et al., 2017).

Regarding the stolons, the data presented here show four different nervous system structures specific to the stolon head: 1) a dorsal concentration of serotonin$^+$ and α-tubulin$^+$ cells close to the anterior end of the stolons head segment that is likely revealing what has been previously interpreted as the stolon's brain (Malaquin, 1893); 2) a pair of circumintestinal connectives that communicate the stolon's brain with the ventral nerve cord (Malaquin, 1893; Weidhase et al., 2016); 3) a dense network of nerve endings in the anterior margin of the stolon head that might be sensory and help the swimming stolon navigate its environment; and 4) a ring of serotonin$^+$ cells at the junction of the stolon's head segment and the segment immediately anterior to it from which a new pygidium develops ventrally before the stolon is released (note that this structure was never observed at the branching points). We believe that these structures, and especially the proposed sensory nerve endings of the anterior head margin,

indicate an active swimming behaviour that might be involved in mating, something that has been previously suggested (Schroeder et al., 2017). Future studies are needed in order to study the structure, development, and function of these structures, as well as to establish whether they are present in all stolon-producing syllids or are phylogenetically restricted.

4.5. Branch anatomy

The main morphological characteristic of *R. multicaudata* is its recursively branching body. These branches emerge laterally from segments throughout the body, and it has been previously documented that they always appear between two parapodia and do not replace them (Glasby et al., 2012). Additionally, those same previous observations mentioned that the internodes in between two branching points greatly vary in length, something that can also be observed in Figure 3D. Why the bifurcation pattern shows irregularities such as these ones remains, hitherto, unknown.

Besides these notes on the general arrangement of the body, our anatomical investigation has revealed that the bifurcated pattern is not just an external morphological feature, but that it also translates into internal anatomy. As a result, we have shown that all longitudinal organ systems bifurcate wherever there is a bifurcation of the exterior body. Moreover, our results also reveal that the ventral nerve cord present in lateral branches is not just an enlarged, previously-existing lateral nerve, but a proper ventral nerve cord that does not replace any of the main segmental nerves. Therefore, it shows the same features that are characteristic of a "complete" annelid ventral nerve cord (Helm et al., 2018; Martín-Durán et al., 2018; M. C. M. Müller, 2006; Schmidbaur et al., 2020; Schmidt-Rhaesa et al., 2016; Starunov et al., 2017). Notably, these results also reveal that the bifurcation of the longitudinal organ systems also results in the formation of what we have called dorsal and ventral muscle bridges.

Taken together, these results indicate that, during development of lateral branches (postembryonic; see unbranched juvenile in Supplementary online material, Figure 1), the

newly emerging lateral divergences of the internal organs must go through the spaces left by the muscles without them disappearing in the process (something that would otherwise result in a discontinuity of the longitudinal muscles in that side of the body). As a result, for each branching point, an original and a derived branch can be identified on the basis of muscle anatomy, which makes it theoretically possible to follow the original (embryonic) anteroposterior axis from the head to the first original terminal end [although the hundreds, or even thousands of branches of each animal make this difficult (Glasby et al., 2012)]. No morphological or functional differences have been observed that would allow one to establish any hierarchy among the branches besides that of the ontogenetic sequence.

5. Conclusions

Our investigations on the arrangement of *R. multicaudata* within the *Petrosia* sponges show that the complex, bifurcating bodies of branched syllids occupy a notable proportion of the canal system of their host sponges. The internal anatomy of *R. multicaudata* is generally comparable to that of other syllids. Thus, the body wall is characterized by a cuticle, a thin epidermal monolayer, and comparatively reduced longitudinal musculature. The circulatory system presents the usual dorsal and ventral longitudinal blood vessels and, although they can sometimes be greatly enlarged, they show little muscularization and lack heart bodies. The digestive tract exhibits the usual syllid-like regionalization and its epithelium varies accordingly in the different regions. However, adult specimens of *R. multicaudata* lack pharyngeal armature and ventricular caeca. The segmental organs and the ventral nerve cord are similar to those found in other syllid species.

The data presented herein also reveals that the lateral branches of *R. multicaudata* contain their corresponding longitudinal organ systems. The latter are entirely continuous throughout

the branching points of the animals, a condition that creates a unique structure here referred to as muscular bridges that theoretically allows one to distinguish the path of the original anteroposterior axis. With these data, we have been able to clarify how the external pattern of bifurcation translates into internal anatomy.

References

Aarle, W. van, Palenstijn, W. J., Beenhouwer, J. De, Altantzis, T., Bals, S., Batenburg, K. J., & Sijbers, J. (2015). The ASTRA Toolbox: A platform for advanced algorithm development in electron tomography. *Ultramicroscopy*, *151*, 35–47. https://doi.org/10.1145/3132847.3132886

Aarle, W. van, Palenstijn, W. J., Cant, J., Janssens, E., Bleichrodt, F., Dabravolski, A., Beenhouwer, J. De, Batenburg, K. J., & Sijbers, J. (2016). Fast and flexible X-ray tomography using the ASTRA toolbox. *Optics Express*, *24*(22), 25129–25147. https://doi.org/10.1364/OE.24.025129

Aguado, M. T., Glasby, C. J., Schroeder, P. C., Weigert, A., & Bleidorn, C. (2015). The making of a branching annelid: an analysis of complete mitochondrial genome and ribosomal data of *Ramisyllis multicaudata*. *Scientific Reports*, *5*, 12072. https://doi.org/10.1038/srep12072

Aguado, M. T., Helm, C., Weidhase, M., & Bleidorn, C. (2015). Description of a new syllid species as a model for evolutionary research of reproduction and regeneration in annelids. *Organisms Diversity and Evolution*, *15*(1), 1–21. https://doi.org/10.1007/s13127-014-0183-5

Aguado, M. T., San Martín, G., & Siddall, M. E. (2012). Systematics and evolution of syllids (Annelida, Syllidae). *Cladistics*, *28*, 234–250. https://doi.org/10.1111/j.1096-

0031.2011.00377.x

Álvarez-Campos, P., San Martín, G., & Aguado, M. T. (2013). A new species and new record of the commensal genus *Alcyonosyllis* Glasby & Watson, 2001 and a new species of *Parahaplosyllis* Hartmann-Schröder, 1990, (Annelida: Syllidae: Syllinae) from Philippines Islands. *Zootaxa*, *3734*(2), 156–168. https://doi.org/10.11646/zootaxa.3734.2.4

Álvarez-Campos, P., Taboada, S., San Martín, G., Leiva, C., & Riesgo, A. (2018). Phylogenetic relationships and evolution of reproductive modes within flattened syllids (Annelida, Syllidae) with the description of a new genus and six new species. *Invertebrate Systematics*, *32*, 224–251. https://doi.org/10.1071/IS17011

Audouin, J. V., & Milne Edwards, H. (1833). Classification des Annélides et description de celles qui habitent les côtes de la France. *Annales Des Sciences Naturelles*, *Ser. 1*(28), 187–247.

Bartolomaeus, T. (1999). Structure, function and development of segmental organs in Annelida. *Hydrobiologia*, *402*(1874), 21–37. https://doi.org/10.1023/A:1003780223216

Beckers, P., Loesel, R., & Bartolomaeus, T. (2013). The nervous systems of basally branching Nemertea (Palaeonemertea). *PLoS ONE*, *8*(6), e66137. https://doi.org/10.1371/journal.pone.0066137

Bleidorn, C., Helm, C., Weigert, A., & Aguado, M. T. (2015). Annelida. In A. Wanninger (Ed.), *Evolutionary developmental biology of invertebrates 2: Lophotrochozoa Spiralia* (1st ed., pp. 193–230). Springer. https://doi.org/10.1007/978-3-7091-1871-9

Boilly, B. (1967). Contribution à l'étude ultrastructurale de la cuticule épidermique et pharyngenne chez une Annélide Polychète (*Syllis amica* Quatrefages). *Journal de Microscopie*, *6*(4), 469–484.

Campoy, A. (1982). Fauna de España. Fauna de anelidos poliquetos de la peninsula iberica. Primera parte. *Publicaciones de Biologia de la Universidad de Navarra*, *7*(1), 1–463.

Cardona, A., Saalfeld, S., Schindelin, J., Arganda-Carreras, I., Preibisch, S., Longair, M., Tomancak, P., Hartenstein, V., & Douglas, R. J. (2012). TrakEM2 software for neural circuit reconstruction. *PLoS ONE*, *7*(6), e38011. https://doi.org/10.1371/journal.pone.0038011

del Castillo, J., Anderson, M., & Smitht, D. S. (1972). Proventriculus of a marine annelid: muscle preparation with the longest recoded sarcomere. *Proceedings of the National Academy of Sciences*, *69*(7), 1669–1672. https://doi.org/10.1073/pnas.69.7.1669

Delgado, J. D., Ocaña, O., Núñez, J., & Talavera, J. A. (1992). Estudio comparado del aparato digestivo de tres especies del género *Syllis* (Plychaeta, Syllidae). *Revista de La Academia Canaria de Ciencias*, *4*(3–4), 131–138.

Fage, L. (1906). Organes segmentaires des Annelides. *Annales Des Sciences Naturelles Zoologie*, *9*(3), 261–410.

Faulwetter, S., Vasileiadou, A., Kouratoras, M., Dailianis, T., & Arvanitidis, C. (2013). Micro-computed tomography: Introducing new dimensions to taxonomy. *ZooKeys*, *263*, 1–45. https://doi.org/10.3897/zookeys.263.4261

Filippova, A., Purschke, G., Tzetlin, A. B., & Müller, M. C. M. (2010). Musculature in polychaetes: comparison of *Myrianida prolifera* (Syllidae) and *Sphaerodoropsis* sp. (Sphaerodoridae). *Invertebrate Biology*, *129*(2), 184–198. https://doi.org/10.1111/j.1744-7410.2010.00191.x

Franke, H.-D. (1999). Reproduction of the Syllidae (Annelida: Polychaeta). *Hydrobiologia*, *402*(2), 39–55. https://doi.org/10.1023/A:1003732307286

Gardiner, S. L. (1992). Polychaeta: general organization, integument, musculature; coelom, and vascular system. In F. W. Harrison & S. L. Gardiner (Eds.), *Microscopic anatomy of invertebrates. (Vol. 7 Annelida)* (pp. 19–52). Wiley-Liss.

Giangrande, A., Licciano, M., & Pagliara, P. (2000). The diversity of diets in Syllidae (Annelida:

Polychaeta). *Cahiers de Biologie Marine*, *41*(1), 55–65. https://doi.org/10.21411/CBM.A.7B8A61C

Glasby, C. J., Schroeder, P. C., & Aguado, M. T. (2012). Branching out: a remarkable new branching syllid (Annelida) living in a *Petrosia* sponge (Porifera: Demospongiae). *Zoological Journal of the Linnean Society*, *164*, 481–497. https://doi.org/10.1111/j.1096-3642.2011.00800.x

Goodrich, E. S. (1900). On the nephridia of Polychaeta. Part III. The Phylodocidae, Syllidae, Amphinomidae, etc., with summary and conclusions. *Quarterly Journal of Microscopical Science*, *43*(172), 699–748.

Goodrich, E. S. (1945). The study of nephridia and genital ducts since 1895. *The Quarterly Journal of Microscopical Science*, *86*(344), 113–392.

Greving, I., Wilde, F., Ogurreck, M., Herzen, J., Hammel, J. U., Hipp, A., Friedrich, F., Lottermoser, L., Dose, T., Burmester, H., Müller, M., & Beckmann, F. (2014). P05 imaging beamline at PETRA III: first results. In R. S. Stuart (Ed.), *Proceedings of SPIE -Developments in X-Ray Tomography IX* (Vol. 9212, 92120O). https://doi.org/10.1117/12.2061768

Grube, A. E. (1840). *Actinien, Echinodermen und Würmer des Adriatischen- und Mittelmeers nach eigenen Sammlungen beschrieben*. J.H. Bon. https://doi.org/10.5962/bhl.title.23025

Haibel, A., Ogurreck, M., Beckmann, F., Dose, T., Wilde, F., Herzen, J., Müller, M., Schreyer, A., Nazmov, V., Simon, M., Last, A., & Mohr, J. (2010). Micro- and nano-tomography at the GKSS Imaging Beamline at PETRA III. *Proceedings of SPIE Optical Engineering + Applications*, *7804*, 8. https://doi.org/10.1117/12.860852

Haswell, W. A. (1921). The proboscis of the Syllidea. Part I. Structure. *Quarterly Journal of Microscopical Science*, *65*, 323–337.

Hausen, H. (2005). Comparative structure of the epidermis in polychaetes (Annelida). In T.

Bartolomaeus & G. Purschke (Eds.), *Morphology, molecules, evolution and phylogeny in Polychaeta and related taxa: Vol. 535/536* (pp. 25–35). Hydrobiologia, Springer. https://doi.org/10.1007/s10750-004-4442-x

Helm, C., Beckers, P., Bartolomaeus, T., Drukewitz, S. H., Kourtesis, I., Weigert, A., Purschke, G., Worsaae, K., Struck, T. H., & Bleidorn, C. (2018). Convergent evolution of the ladder-like ventral nerve cord in Annelida. *Frontiers in Zoology*, *15*(36), 1–17. https://doi.org/10.1101/378661

Helm, C., & Capa, M. (2015). Comparative analyses of morphological characters in Sphaerodoridae and allies (Annelida) revealed by an integrative microscopical approach. *Frontiers in Marine Science*, *1*, 1–15. https://doi.org/10.3389/fmars.2014.00082

Imajima, M., & Hartman, O. (1964). The polychaetous annelids of Japan. *Occasional Papers of the Allan Hancock Foundation*, *26*(Part I), 1–237.

Izuka, A. (1912). The errantiate Polychaeta of Japan. *Journal of the College of Science, Imperial University of Tokyo*, *30*(2), 1–262. https://doi.org/10.1126/science.ns-18.446.109

Jeuniaux, C. (1969). Nutrition and Digestion. In *Chemical zoology. Volume 4: Annelida, Echiuria, and Sipuncula* (pp. 69–91). Academic Press, Inc. https://doi.org/10.1016/b978-0-12-395537-1.50008-7

Jumars, P. A., Dorgan, K. M., & Lindsay, S. M. (2015). Diet of worms emended: An update of polychaete feeding guilds. *Annual Review of Marine Science*, *7*, 497–520. https://doi.org/10.1146/annurev-marine-010814-020007

Kuper, M. (2001). *Ultrastrukturuntersuchungen der Segmentalorgane, der Spermien und der Brutpflegestrukturen innerhalb der Syllidae (Annelida: Polychaeta)*. [Doctoral disseration, Osnabrück University, Osnabrück, Germany]. Retrieved from: https://repositorium.ub.uni-osnabrueck.de/handle/urn:nbn:de:gbv:700-2002021316

Lytaev, P., Hipp, A., Lottermoser, L., Herzen, J., Greving, I., Khokhriakov, I., Meyer-Loges, S., Plewka, J., Burmester, J., Caselle, M., Vogelgesang, M., Chilingaryan, S., Kopmann, A., Balzer, M., Schreyer, A., & Beckmann, F. (2014). Characterization of the CCD and CMOS cameras for grating-based phase-contrast tomography. *Proceedings of SPIE Optical Engineering + Applications*, *9212*, 10. https://doi.org/10.1117/12.2061389

Malaquin, A. (1893). *Recherches sur les syllidiens: Morphologie, anatomie, reproduction, développement*. L. Danel.

Martín-Durán, J. M., Pang, K., Børve, A., Lê, H. S., Furu, A., Cannon, J. T., Jondelius, U., & Hejnol, A. (2018). Convergent evolution of bilaterian nerve cords. *Nature*, *553*(7686), 45–50. https://doi.org/10.1038/nature25030

Martin, D., Aguado, M. T., Fernández Álamo, M.-A., Britayev, T. A., Böggemann, M., Capa, M., Faulwetter, S., Fukuda, M. V., Helm, C., Angelica, M., Petti, V., Ravara, A., & Teixeira, M. A. L. (2021). On the diversity of Phyllodocida (Annelida: Errantia), with a focus on Glyceridae, Goniadidae, Nephtyidae, Polynoidae, Sphaerodoridae, Syllidae, and the Holoplanktonic families. *Diversity*, *13*, 131. https://doi.org/10.3390/d13030131

McIntosh, W. C. (1879). On a remarkably branched *Syllis* dredged by H.M.S. Challenger. *Journal of the Linnean Society London*, *14*, 720–724.

McIntosh, W. C. (1885). Report on the Annelida Polychaeta collected by H.M.S. Challenger during the years 1873-1876. *Challenger Reports*, *12*, 189–208.

Michel, C. (1974). L'armature de la trompe de *Syllis cornuta* Rathke (Étude histochimique et biochimique). *Annales d'Histochimie*, *19*, 173–185.

Mill, P. J. (1978). *Physiology of annelids*. Academic Press, Inc.

Moosmann, J., Ershov, A., Weinhardt, V., Baumbach, T., Prasad, M., LaBonne, C., Xiao, X., Kashef, J., & Hoffmann, R. (2014). Time-lapse X-ray phase-contrast microtomography for

in vivo imaging and analysis of morphogenesis. Nature Protocols, 9, 294 – 304. *Nature Protocols*, *9*, 294–304. https://doi.org/10.1038/nprot.2014.033

Müller, M. C. M. (2006). Polychaete nervous systems: Ground pattern and variations - cLS microscopy and the importance of novel characteristics in phylogenetic analysis. *Integrative and Comparative Biology*, *46*(2), 125–133. https://doi.org/10.1093/icb/icj017

Müller, O. F. (1778). *Zoologia Danica seu animalium Daniae et Norvegiae rariorum ac minus notorum descriptiones et historia. Volumen secundum.* N. Möller.

Oka, A. (1895). Über die Knospungsweise bei *Syllis ramosa*. *Zoologischer Anzeiger*, *18*, 462–464.

Okada, Y. K. (1937). La stolonisation et les caracteres sexuels du stolon chez les Syllidiens Polychetes (Études sur les Syllidiens III). *Japanese Journal of Zoology*, *7*, 441–490.

Orrhage, L., & Müller, M. C. M. (2005). Morphology of the nervous system of Polychaeta (Annelida). *Hydrobiologia*, *535/536*, 79–111. https://doi.org/10.1007/s10750-004-4375-4

Palenstijn, W. J., Batenburg, K. J., & Sijbers, J. (2011). Performance improvements for iterative electron tomography reconstruction using graphics processing units (GPUs). *Journal of Structural Biology*, *176*(2), 250–253. https://doi.org/10.1051/forest

Pamungkas, J., Glasby, C. J., Read, G. B., Wilson, S. P., & Costello, M. J. (2019). Progress and perspectives in the discovery of polychaete worms (Annelida) of the world. *Helgoland Marine Research*, *73*(4), 1–10. https://doi.org/10.1186/s10152-019-0524-z

Parapar, J., Candás, M., Cunha-Veira, X., & Moreira, J. (2017). Exploring annelid anatomy using micro-computed tomography: A taxonomic approach. *Zoologischer Anzeiger*, *270*, 19–42. https://doi.org/10.1016/j.jcz.2017.09.001

Parapar, J., Caramelo, C., Candás, M., Cunha-Veira, X., & Moreira, J. (2019). An integrative

approach to the anatomy of *Syllis gracilis* Grube, 1840 (Annelida) using micro-computed X-ray tomography. *PeerJ*, *e7251*. https://doi.org/10.7717/peerj.7251

Pleijel, F. (2001). Syllidae, Grube, 1850. In G. W. Rouse & F. Pleijel (Eds.), *Polychaetes* (pp. 102–105). Oxford University Press.

Purschke, G., & Müller, M. C. M. (2006). Evolution of body wall musculature. *Integrative and Comparative Biology*, *46*(4), 497–507. https://doi.org/10.1093/icb/icj053

Quatrefages, M. A. de. (1866). *Histoire naturelle des Annelés marins et d'eau douce. Annélides et Géphyriens. Volume 2*. Librarie Encyclopédique de Roret.

Read, G. (2001). Unique branching worm found in New Zealand. *Biodiversity Update (NIWA)*, *4*, 1 (only).

Ribeiro, R. P., Ponz-Segrelles, G., Helm, C., Egger, B., Bleidorn, C., & Aguado, M. T. (2020). A new species of *Syllis* including transcriptomic data and an updated phylogeny of Syllinae (Annelida: Syllidae). *Marine Biodiversity*, *50*(31), 16. https://doi.org/10.1007/s12526-020-01046-y

Rouse, G. W., & Pleijel, F. (2001). *Polychaetes*. Oxford University Press.

San Martín, G. (2003). *Fauna Ibérica, Volume 21: Annelida: Polychaeta II: Syllidae*. Museo Nacional de Ciencias Naturales.

San Martín, G., & Aguado, M. T. (2012). Contribution of scanning electron microscope to the study of morphology, biology, reproduction, and phylogeny of the family Syllidae (Polychaeta). In V. Kazmiruk (Ed.), *Scanning Electron Microscopy* (pp. 129–146). InTech Publisher. https://doi.org/10.5772/34681

San Martín, G., & Aguado, M. T. (2014). Family Syllidae. In A. Schmidt-Rhaesa (Ed.), *Handbook of Zoology. Annelida: Polychaetes* (pp. 1–68). De Gruyter.

Saulnier-Michel, C. (1992). Polychaeta: digestive system. In F. W. Harrison & S. L. Gardiner (Eds.), *Microscopic Anatomy of Invertebrates (Vol. 7 Annelida)* (pp. 53–69). Wiley-Liss.

Schindelin, J., Arganda-Carreras, I., Frise, E., Kaynig, V., Longair, M., Pietzsch, T., Preibisch, S., Rueden, C., Saalfeld, S., Schmid, B., Tinevez, J. Y., White, D. J., Hartenstein, V., Eliceiri, K., Tomancak, P., & Cardona, A. (2012). Fiji: An open-source platform for biological-image analysis. *Nature Methods*, *9*(7), 676–682. https://doi.org/10.1038/nmeth.2019

Schmidbaur, H., Schwaha, T., Franzkoch, R., Purschke, G., & Steiner, G. (2020). Within-family plasticity of nervous system architecture in Syllidae (Annelida, Errantia). *Frontiers in Zoology*, *17*(20), 1–44. https://doi.org/10.1186/s12983-020-00359-9

Schmidt-Rhaesa, A., Harzsch, S., & Purschke, G. (2016). *Structure and Evolution of Invertebrate Nervous Systems*. Oxford University Press. https://doi.org/10.1017/CBO9781107415324.004

Schroeder, P. C., Aguado, M. T., Malpartida, A., & Glasby, C. J. (2017). New observations on reproduction in the branching polychaetes, *Ramisyllis multicaudata* and *Syllis ramosa* (Annelida: Syllidae: Syllinae). *Journal of the Marine Biological Association of the United Kingdom*, *97*(5), 1167–1175. https://doi.org/10.1017/S002531541700039X

Starunov, V. V., Voronezhskaya, E. E., & Nezlin, L. P. (2017). Development of the nervous system in *Platynereis dumerilii* (Nereididae, Annelida). *Frontiers in Zoology*, *14*(1), 1–20. https://doi.org/10.1186/s12983-017-0211-3

Tzetlin, A. B., & Filippova, A. V. (2005). Muscular system in polychaetes (Annelida). *Hydrobiologia*, *535*(1), 113–126. https://doi.org/10.1007/s10750-004-1409-x

Tzetlin, A. B., & Purschke, G. (2005). Pharynx and intestine. In T. Bartolomaeus & G. Purschke (Eds.), *Morphology, molecules, evolution and phylogeny in Polychaeta and related taxa: Vol. 535/536* (pp. 199–225). Hydrobiologia, Springer. https://doi.org/10.1007/s10750-

004-1431-z

Tzetlin, A. B., Zhadan, A., Ivanov, I., Müller, M. C. M., & Purschke, G. (2002). On the absence of circular muscle elements in the body wall of *Dysponetus pygmaeus* (Chrysopetalidae, "Polychaeta", Annelida). *Acta Zoologica*, *83*(1), 81–85. https://doi.org/10.1046/j.1463-6395.2002.00104.x

Weidhase, M., Beckers, P., Bleidorn, C., & Aguado, M. T. (2016). On the role of the proventricle region in reproduction and regeneration in *Typosyllis antoni* (Annelida: Syllidae). *BMC Evolutionary Biology*, *16*(1), 196. https://doi.org/10.1186/s12862-016-0770-5

Weidhase, M., Beckers, P., Bleidorn, C., & Aguado, M. T. (2017). Nervous system regeneration in *Typosyllis antoni* (Annelida: Syllidae). *Zoologischer Anzeiger*, *269*, 57–67. https://doi.org/10.1016/j.jcz.2017.07.004

Weidhase, M., Bleidorn, C., & Helm, C. (2014). Structure and anterior regeneration of musculature and nervous system in *Cirratulus* cf. *cirratus* (Cirratulidae, Annelida). *Journal of Morphology*, *275*(12), 1418–1430. https://doi.org/10.1002/jmor.20316

Wilde, F., Ogurreck, M., Greving, I., Hammel, J. U., Beckmann, F., Hipp, A., Lottermoser, L., Khokhriakov, I., Lytaev, P., Dose, T., Burmester, H., Müller, M., & Schreyer, A. (2016). Micro-CT at the imaging beamline P05 at PETRA III. *AIP Conference Proceedings*, *1741*, 030035. https://doi.org/10.1063/1.4952858

Acknowledgments

This research was supported by MINECO/ERDF, UE funds (Grant: CGL2015-63593-P, "Macroevolutionary transitions in Syllidae" project, PI: MTA) and the PETRA III Beamline project, Deutsches Elektronen-Synchrotron ("Living in a labyrinth: Insights into the interaction

between a branching annelid and its host sponge", PI: MTA). GP-S is supported by the "Contratos Predoctorales para la Formación de Doctores 2016" program of MINECO, Spain (code: BES-2016-076419), co-financed by the European Social Found. RPR is supported by the program "Contratos predoctorales para Formación de Personal Investigador, FPI-UAM," Universidad Autónoma de Madrid. GP-S and MTA would like to thank the Museum and Art Gallery of the Northern Territory for hosting their visits as part of the visiting scientist program in December 2017 and July 2018. We thank Paul Schroeder, Christian Fischer, and especially Christoph Bleidorn for all their help and interesting views on the topics covered in this article.

Conflict of Interests

The authors declare no competing interests.

Author Contributions

Guillermo Ponz-Segrelles: Conceptualization; investigation; data curation; visualization; writing – original draft. **Christopher J. Glasby:** Investigation; resources; writing-review and editing. **Conrad Helm:** Investigation; data curation; visualization; writing-review and editing. **Patrick Beckers:** Investigation; data curation; visualization; writing-review and editing. **Jörg U. Hammel:** Methodology; investigation; data curation; visualization; writing-review and editing. **Rannyele Passos Ribeiro:** Investigation; visualization; writing-review and editing. **M. Teresa Aguado:** Conceptualization; investigation; data curation; supervision; project administration; funding acquisition; writing-review and editing.

Data Availability Statement

The data that support the findings of this study are available from the corresponding authors upon request.

Figure Legends

Figure 1 *Ramisyllis multicaudata,* living specimens. A, Fragment of the anterior end of an individual dissected out of its host sponge. The head (bottom left) is followed by all the usual syllid foregut structures (most notably, the pharynx, the cream-coloured proventricle, and the ventricle) up to the first branching point. Bifurcation of the gut can be seen by transparency. **B**, In-situ image of a *Petrosia* sp. sponge where several posterior ends of one specimen of *R. multicaudata* can be seen as white lines crawling on the sponge's surface. **C**, Small fraction of a single living specimen dissected out of it host sponge as seen through the stereomicroscope. Some dislodged fragments of sponge tissue can also be seen. Scale bar: 1 mm

Figure 2 *Ramisyllis multicaudata,* development of the branched body. Left: Early post-embryonic individual showing a single anteroposterior (AP) axis. At this stage, individuals show the regular bilateral pattern of annelids (see Supplementary online material, Figure 1). Middle: shortly after the previous stage, a lateral branch emerges from a pre-existing midbody segment. As far as it is known, the position and orientation of this first branch and all the subsequent ones does not follow any pattern. Right: Adult individuals present a large and complicated body with high-order branching. The lack of regular bifurcation patterns creates an asymmetric body. Note that this drawing is an idealized version of an adult individual. Real individuals are much larger and have many more branches than depictured here.

Figure 3 *Ramisyllis multicaudata* within a fragment of its host sponge, micro-computed tomography three-dimensional reconstructions. A, Transparent sponge volume (blue) showing the disposition of the annelid branches (yellow) within the canal system (see Supplementary online material, Animated GIF 1). **B**, Different view of the same reconstruction

where the right half of the sponge tissue has been computationally removed to show the complex arrangement of the branches within the canal system (see Supplementary online material, Video 2 and Animated GIF 2). **C**, Frontal view of B. Sponge tissue has been coloured in beige; annelid tissue has been coloured in red. **D**, Architecture of the branch network of the same specimen of *R. multicaudata* created by reducing each branch to its midline. Note that the reconstructions show several non-connected pieces despite each sponge hosting only one specimen of *R. multicaudata*. These pieces were probably connected outside of the scanned fragment of the sponge, which was too big to be scanned entirely.

Figure 4 *Ramisyllis multicaudata,* selection of histological cross sections at different levels of the body from anterior to posterior. A, section at the level of the anterior third of the pharynx region. **B**, Section at the level of the proventricle region. Top left rectangle showing a detail of a different section showing the proventricular plates. **C**, Section at the level of the ventricle region. **D**, Section at the level of the anterior portion of the intestine, immediately posterior to the ventricle. **E**, Section at the level of the first bifurcation. Note the bifurcation of all longitudinal structures and that the left ventral blood vessel appears particularly large because it is in diagonal section due to the angle of the emerging branch. **F**, Section at the level of the intestine immediately posterior to the first bifurcation. Abbreviations: dbv, dorsal blood vessel; dlm, dorsal longitudinal muscle; int, intestine; phx, pharynx; prv, proventricle; pvp, proventricular plates; sgo, segmental organ; sgl, salivary gland; vbv, ventral blood vessel; vlm, ventral longitudinal muscle; vnc, ventral nerve cord; vtr, ventricle. Scale bar: 200 μm.

Figure 5 *Ramisyllis multicaudata,* transmission electron micrographs of the body wall and gut epithelium. A, Ventral body wall. Pink coloured area marks the cuticle separating the body (top) form its surrounding environment (bottom). **B**, Detail of the body's surface. Pink coloured area marks the cuticle separating the body (right) form its surrounding environment (left). Note the abundance of microvilli that protrude outside the cuticular matrix. **C**, Lumen of the

posterior intestine (coloured in yellow). **D**, Detail of the posterior intestine epithelium showing the cilia and microvilli of its surface. Abbreviations: cil, cilia; cut, cuticle; miv, microvilli; pil, posterior intestine lumen. Scale bars: 10 µm (A, C); 1 µm (B, D).

Figure 6 *Ramisyllis multicaudata,* immunohistochemical stainings of musculature and nervous system of stolons and pygidia. A, Z projection of a cLSM image stack of a non-stolon posterior end in which cell nuclei and tubulinergic cells have been stained, dorsal view. White arrowhead points to the position of stained cilia in the posterior end of the gut. **B**, Z projection of a cLSM image stack of a regenerating posterior end in which tubulinergic cells have been stained, dorsal view. White arrowhead points to the position of stained cilia in the posterior end of the regenerating gut; dashed white line indicates the position of the injury. **C**, Z projection of a cLSM image stack of the anterior portion of a developing stolon (bottom) still attached to the stalk (top) in which cell nuclei, serotonergic cells, and myosin filaments have been stained, ventral view; anterior up. Dashed white line indicates the anterior margin of the developing stolon head; white asterisks indicate the position of the stolon's eyes; white arrowhead pints to the position of the stolon brain; golden arrowhead points to the position of the ventrally growing pygidium immediately anterior to the stolon's head. **D**, Z projection of a cLSM image stack of the anterior half of a mature (released) male stolon in which tubulinergic and serotoninergic cells have been stained, dorsal view; anterior up. White asterisks indicate the position of the stolon's eyes; golden arrowhead points to the position of the stolon's brain; I-IV indicate the four main segmental nerves. Bottom-left corner shows the same Z projection but based on a reduced image stack. White arrowheads indicate the position of the circumintestinal connectives; golden line indicates the anterior margin of the stolons head. Scale bars: 50 µm.

Figure 7 *Ramisyllis multicaudata,* three-dimensional reconstruction of histological sections of the anterior end. A, Ventral view of the complete model from the head (right) to the first

branching point (left). Grey lines indicate the body's surface, cirri, and antennae, based on a live image of a different individual. Note that musculature (dark grey) is only shown at the branching point for visualization purposes. **B**, Enlarged view of the branching point, ventral view. Small arrow points to the muscle bridge (dark grey) dorsally crossing over the ventral nerve cord (green). **C**, Enlarged view of the branching point, dorsal view. Small arrow points to the muscle bridge (dark grey) dorsally crossing over the digestive tube (red). Note that only the ventral blood vessel is represented since it is remarkably bigger than the dorsal vessel.

Figure 8 *Ramisyllis multicaudata,* Z projection of a cLSM image stacks of immunohistochemical stainings of musculature and nervous system at the branching point. **A** and **B**, Anti-f-actin stainings confirming the presence of muscle bridges (see text) in one of the three branches coming out of a branching point. Dashed lines mark the position of the muscle bridges. **C**, Nervous system staining reveals the presence of the numerous serotonergic neurons characteristic of the ventral nerve cord in all three branches coming out of a branching point. Arrows point to the position of the ventral nerve cord; white arrowheads point to some of the serotonergic neurons; blue arrowheads point to the pairs of segmental neurite bundles that emerge from the ventral nerve cord but show no serotonergic neurons (note that the emerging VNC does not substitute any of the segmental neurite bundles). **D**, Nervous system staining in a recently emerged branch bearing a posterior end, showing the presence of a complete ventral nerve cord emerging from the original one (see discussion). Scale bars: 50 μm.

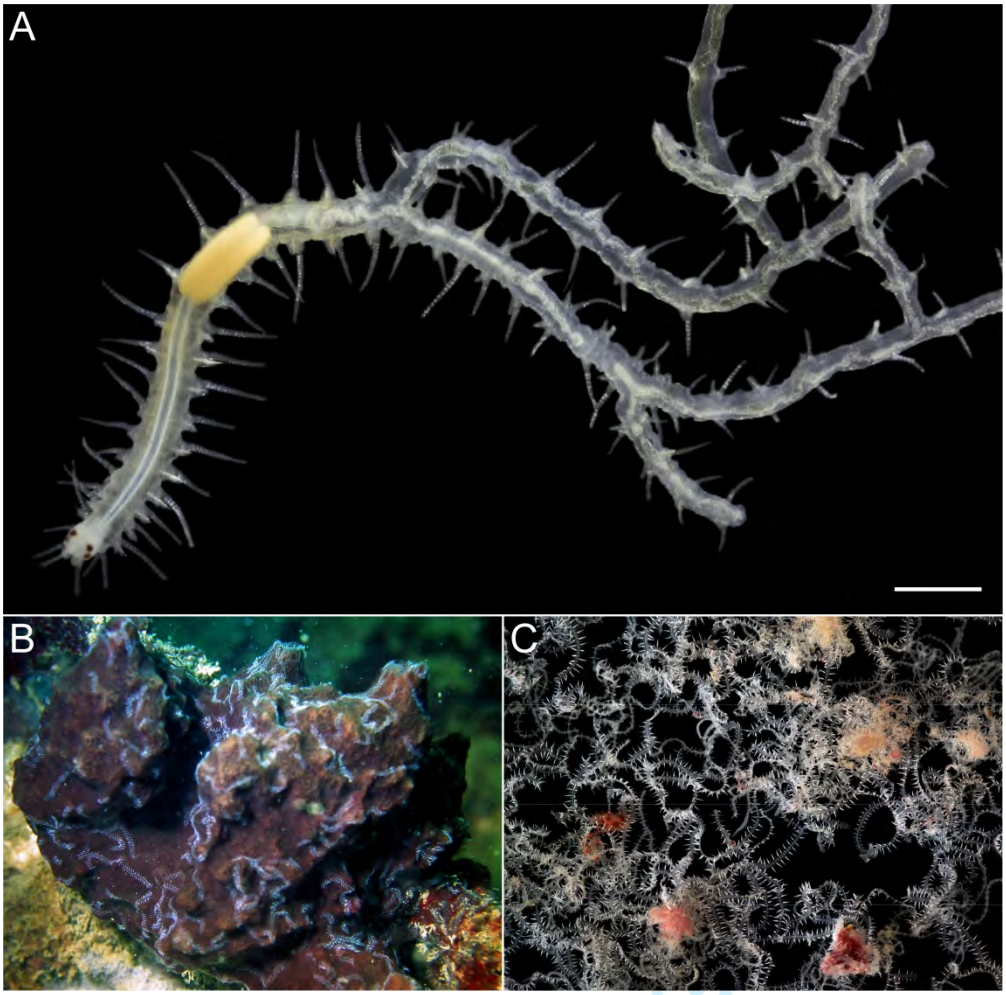

Living specimens of *Ramisyllis multicaudata*. A, Fragment of the anterior end of an individual dissected out of its host sponge. The head (bottom left) is followed by all the usual syllid foregut structures (most notably, the pharynx, the cream-coloured proventricle, and the ventricle) up to the first branching point. Bifurcation of the gut can be seen by transparency. B, In-situ image of a *Petrosia* sp. sponge where several posterior ends of one specimen of *R. multicaudata* can be seen as white lines crawling on the sponge's surface. C, Small fraction of a single living specimen dissected out of it host sponge as seen through the stereomicroscope. Some dislodged fragments of sponge tissue can also be seen. Scale bar: 1 mm

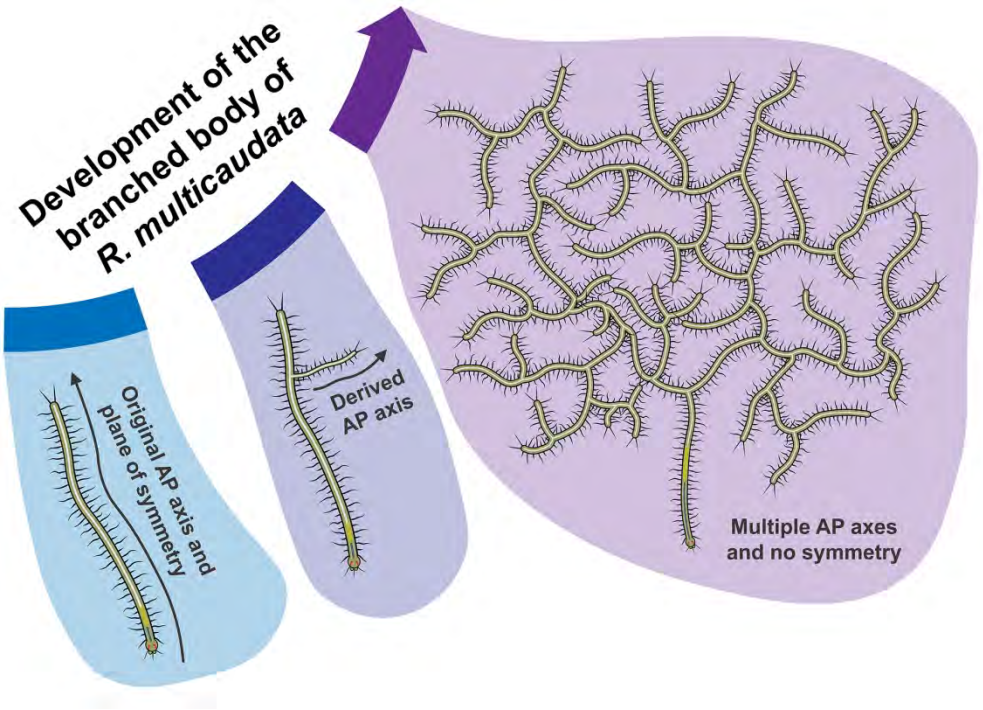

Development of the branched body of *R. multicaudata*. Left: Early post-embryonic individual showing a single anteroposterior (AP) axis. At this stage, individuals show the regular bilateral pattern of annelids (see Supplementary Figure 1). Middle: shortly after the previous stage, a lateral branch emerges from a pre-existing midbody segment. As far as it is known, the position and orientation of this first branch and all the subsequent ones doesn't follow any pattern. Right: Grown individuals present a big and complicated body with high-order branching. The lack of regular bifurcation patterns creates an asymmetric body. Note that this drawing is an idealized version of an adult individual. Real individuals are much larger and have many more branches than depictured here.

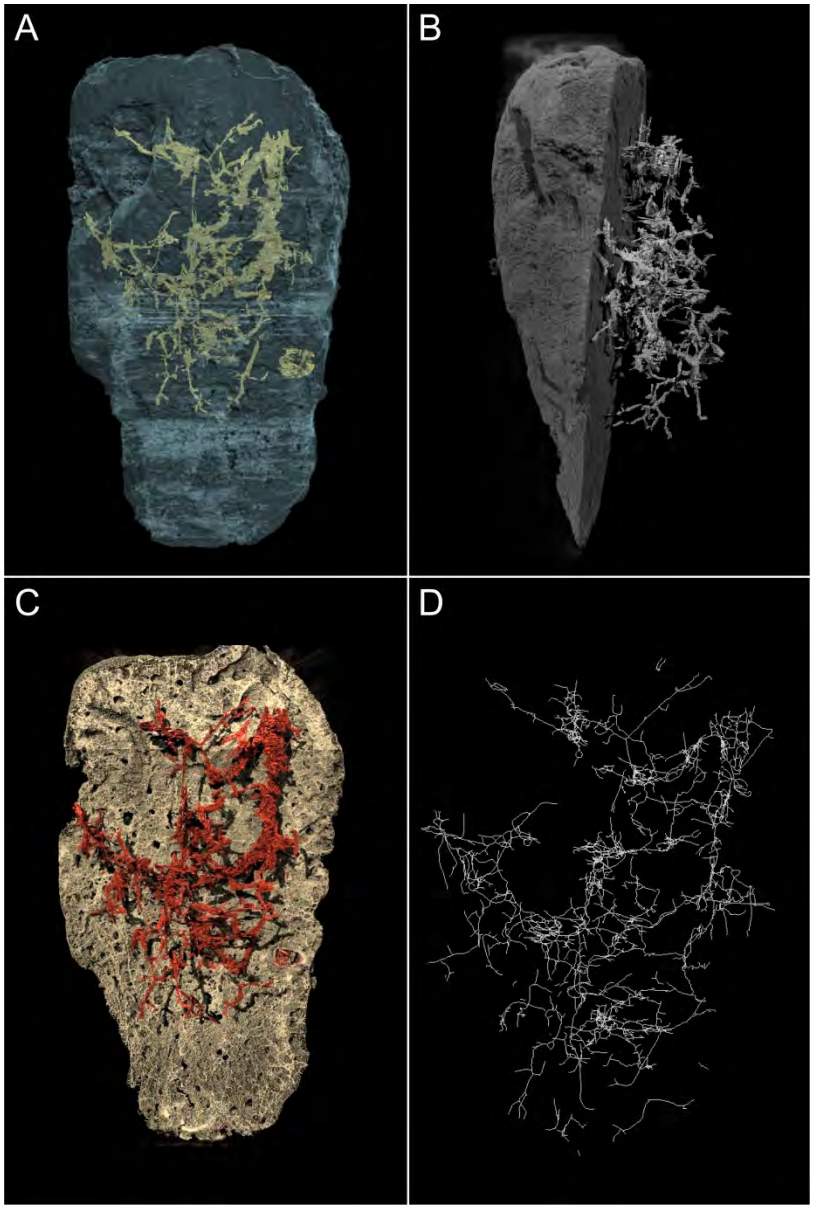

Micro-computed tomography three-dimensional reconstructions of *Ramisyllis multicaudata* within a fragment of its host sponge. A, Transparent sponge volume (blue) showing the disposition of the annelid branches (yellow) within the canal system (see Supplementary Animated GIF 1). B, Different view of the same reconstruction where the right half of the sponge tissue has been computationally removed to show the complex arrangement of the branches within the canal system (see Supplementary Video 2 and Supplementary Animated GIF 2). C, Frontal view of B. Sponge tissue has been coloured in beige; annelid tissue has been coloured in red. D, Architecture of the branch network of the same specimen of R. multicaudata created by reducing each branch to its midline. Note that the reconstructions show several non-connected pieces despite each sponge hosting only one specimen of *R. multicaudata*. These pieces were probably connected outside of the scanned fragment of the sponge, which was too big to be scanned entirely.

A

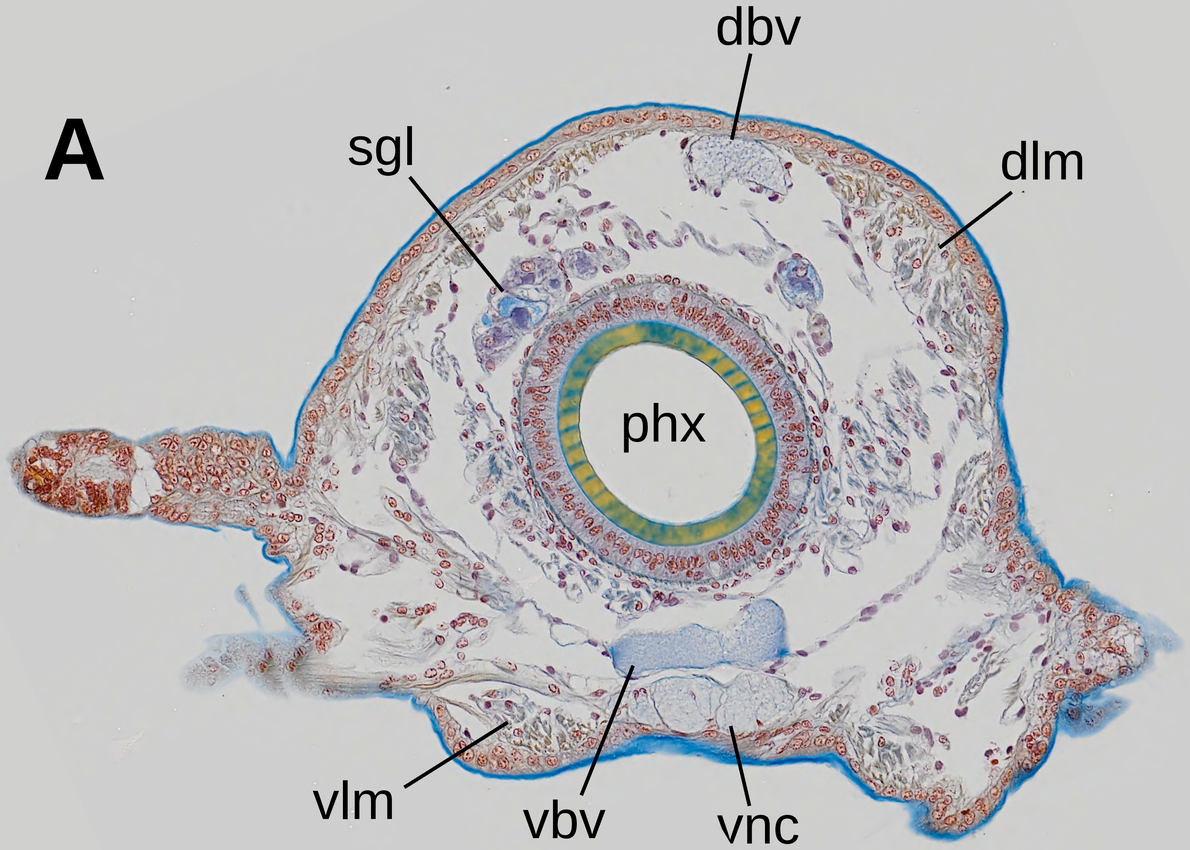

B

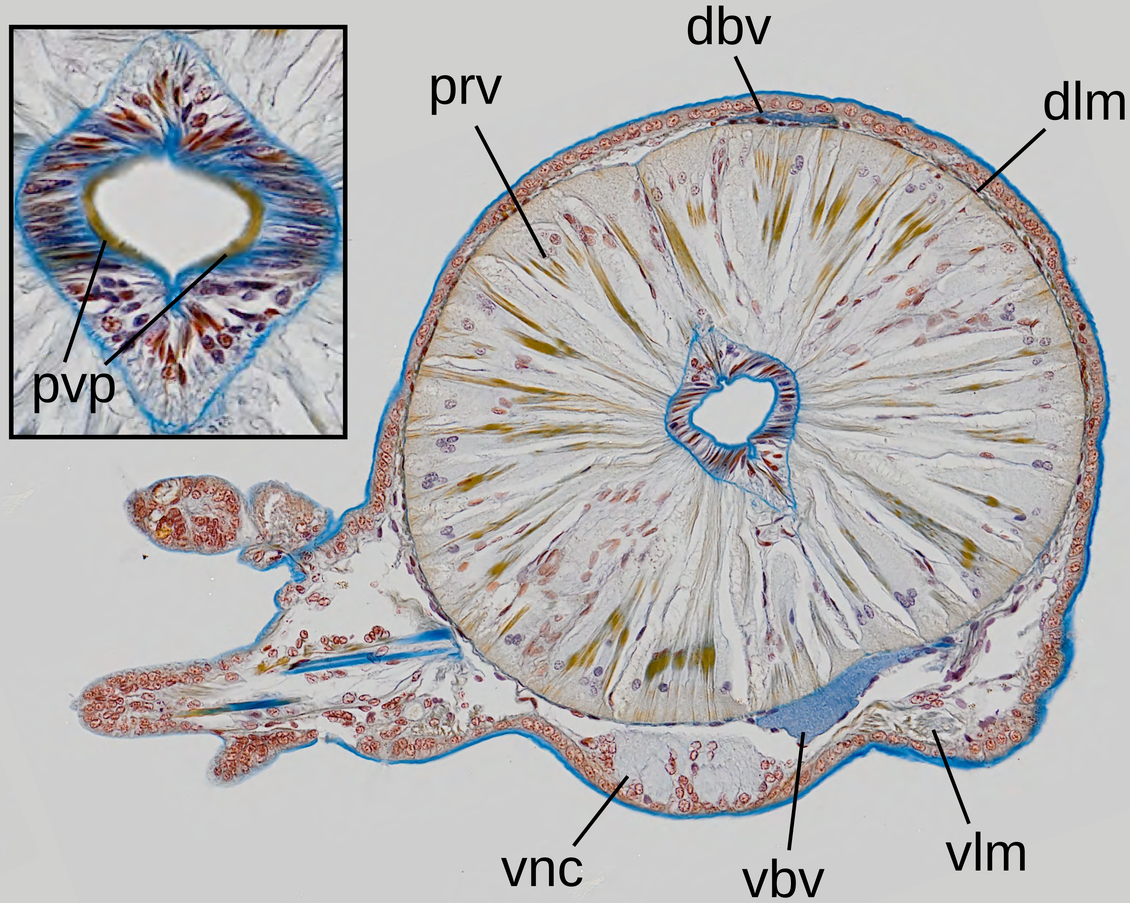

C

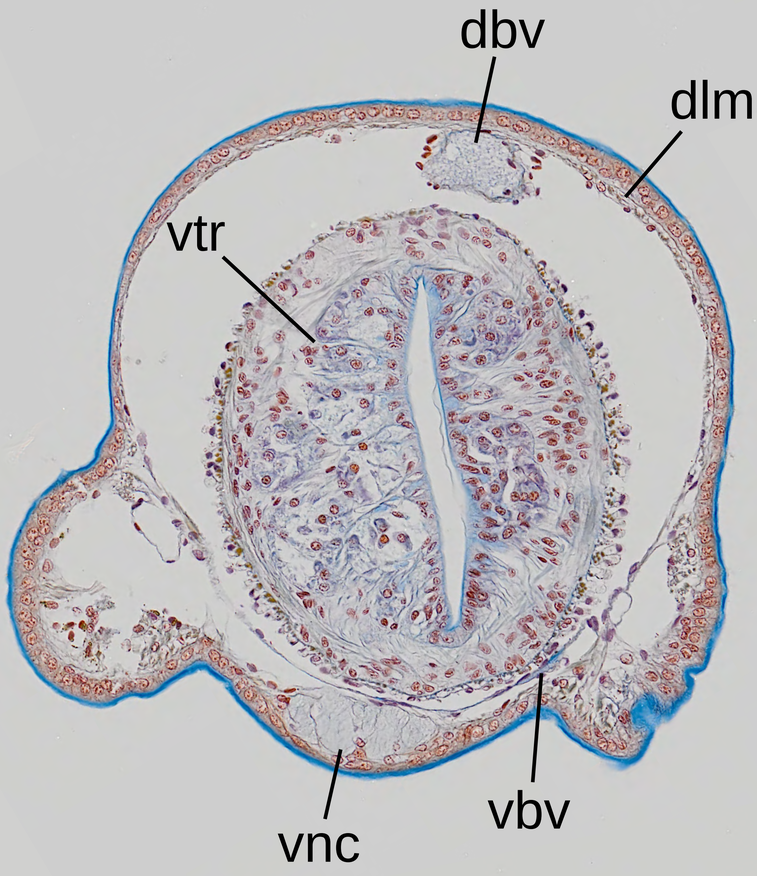

D

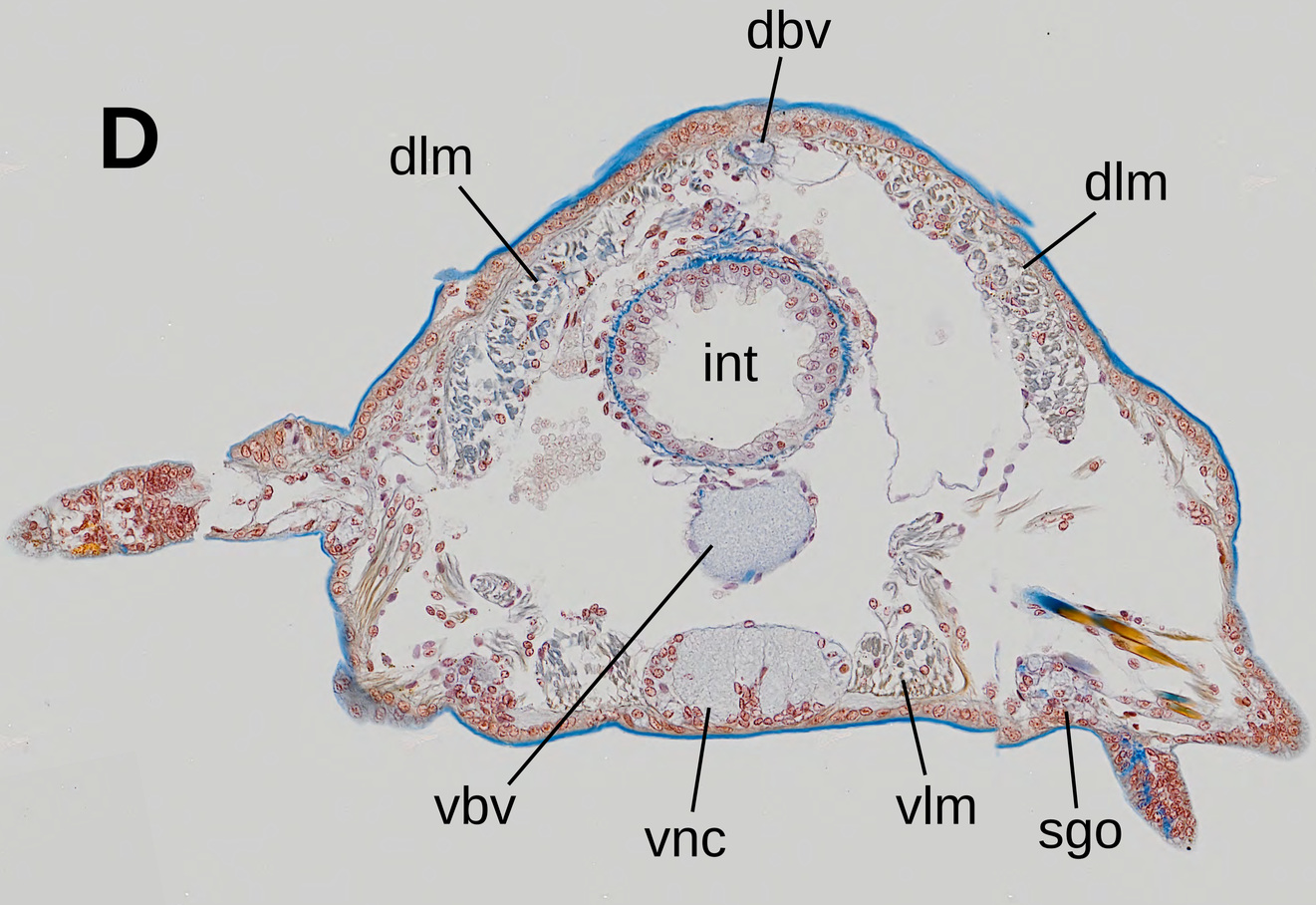

E

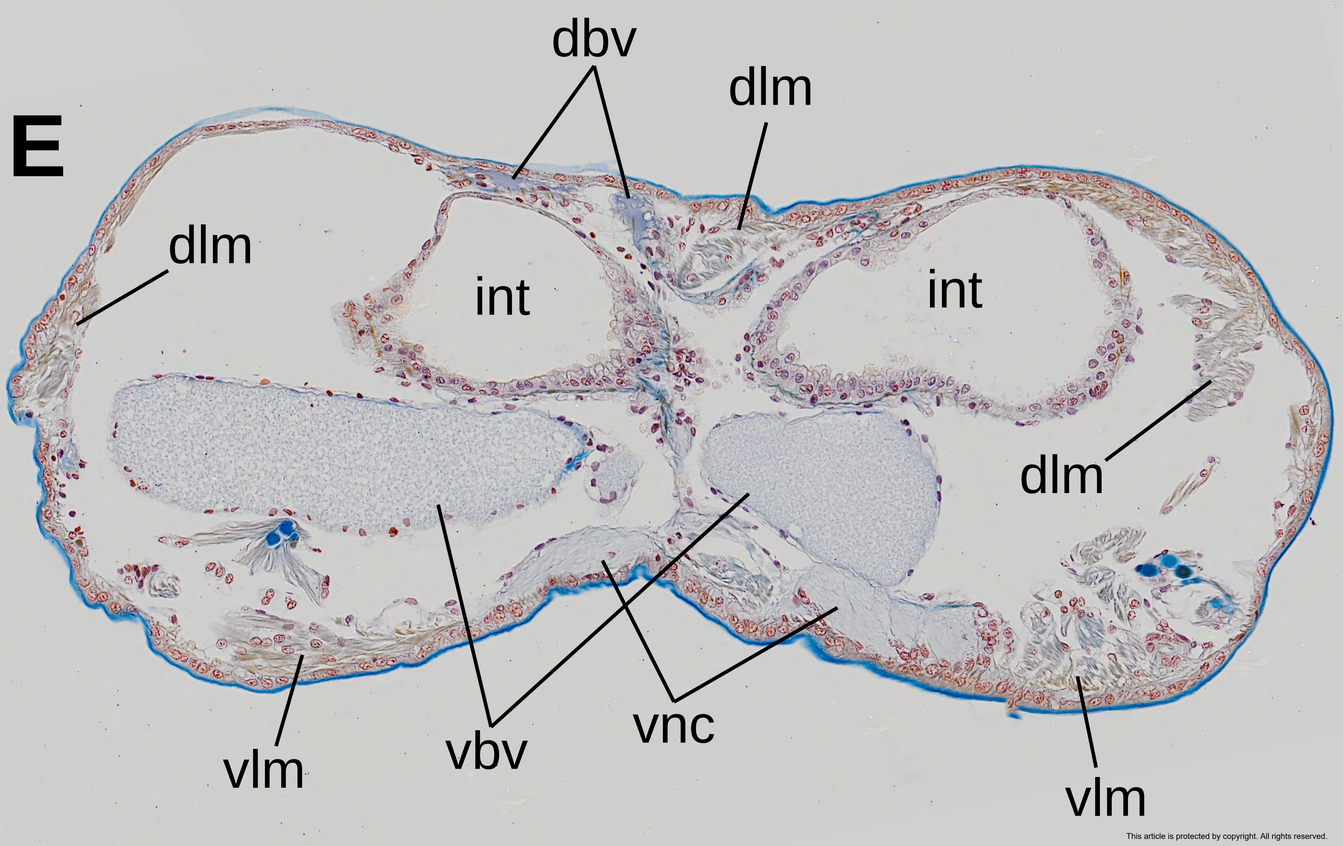

F

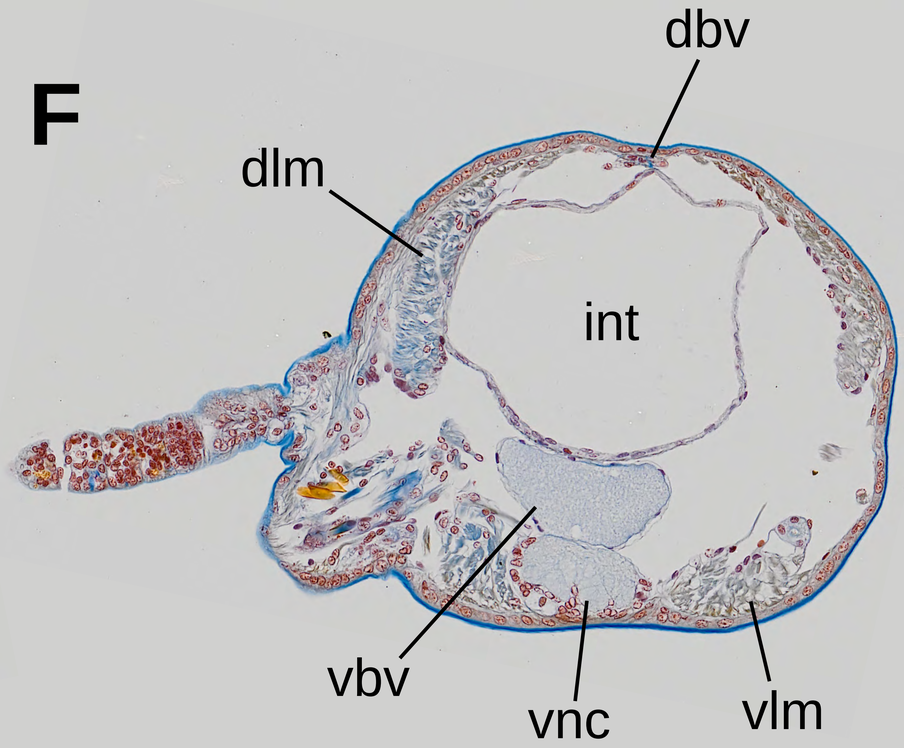

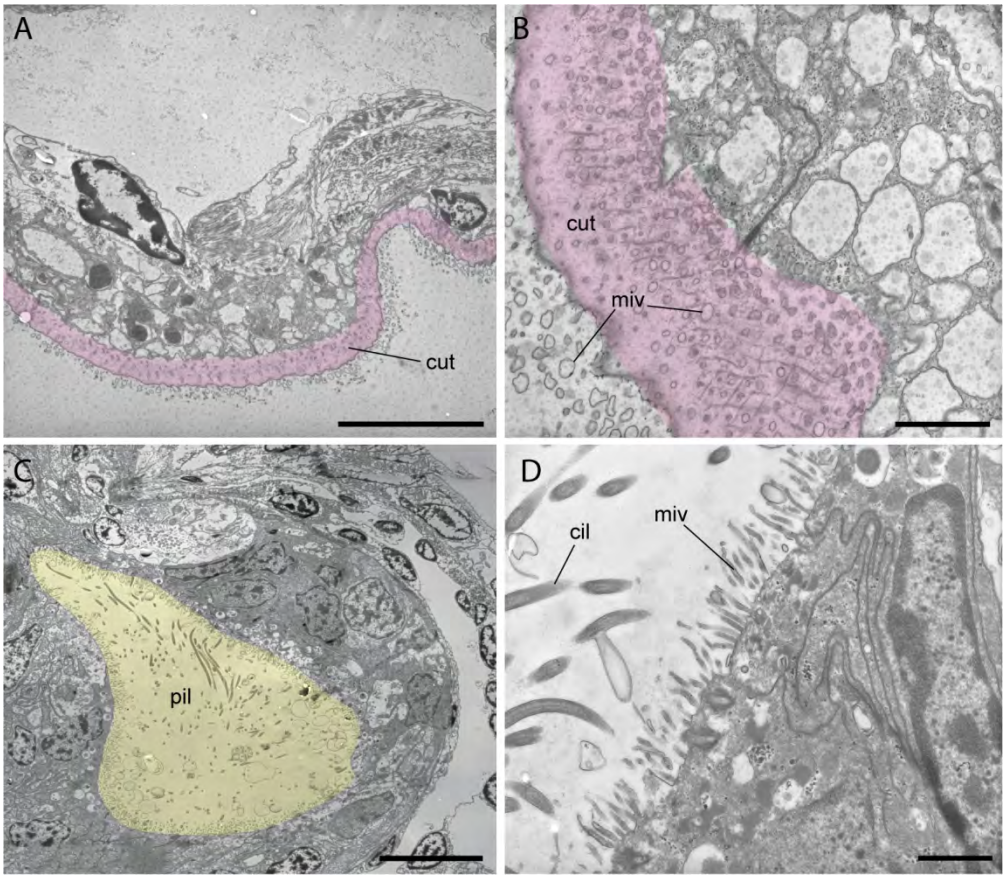

TEM images of the body wall and gut epithelium. A, Ventral body wall. Pink coloured area marks the cuticle separating the body (top) form its surrounding environment (bottom). B, Detail of the body's surface. Pink coloured area marks the cuticle separating the body (right) form its surrounding environment (left). Note the abundance of microvilli that protrude outside the cuticular matrix. C, Lumen of the posterior intestine (coloured in yellow). D, Detail of the posterior intestine epithelium showing the cilia and microvilli of its surface. Abbreviations: cil, cilia; cut, cuticle; miv, microvilli; pil, posterior intestine lumen. Scale bars: 10 µm (A, C); 1 µm (B, D).

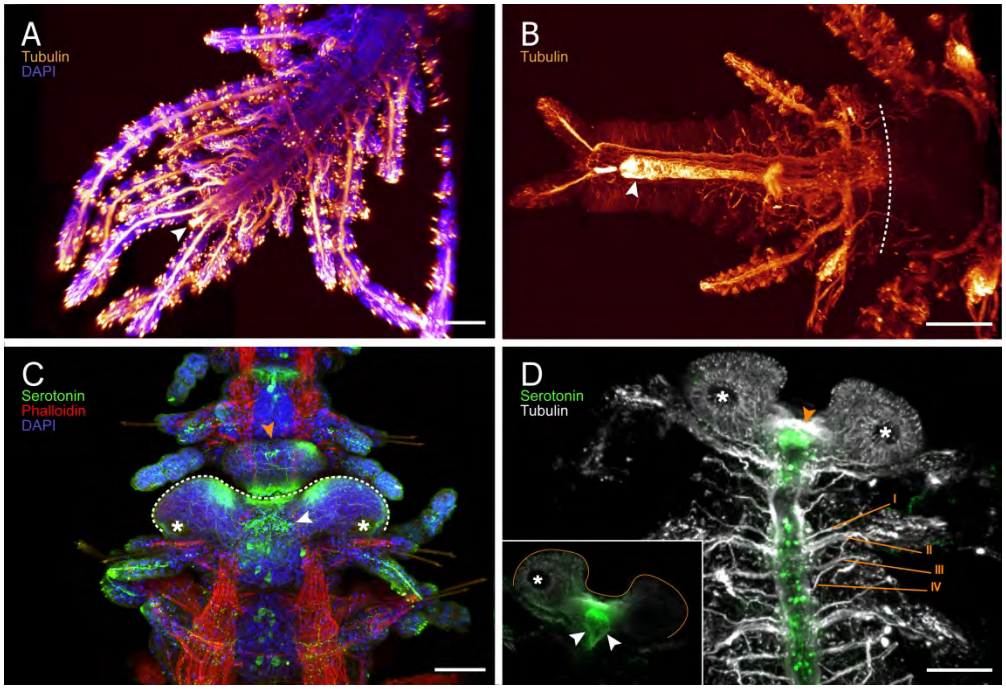

Immunohistochemical stainings of musculature and nervous system of stolons and pygidia. A, Z projection of a cLSM image stack of a non-stolon posterior end in which cell nuclei and tubulinergic cells have been stained, dorsal view. White arrowhead points to the position of stained cilia in the posterior end of the gut. B, Z projection of a cLSM image stack of a regenerating posterior end in which tubulinergic cells have been stained, dorsal view. White arrowhead points to the position of stained cilia in the posterior end of the regenerating gut; dashed white line indicates the position of the injury. C, Z projection of a cLSM image stack of the anterior portion of a developing stolon (bottom) still attached to the stalk (top) in which cell nuclei, serotonergic cells, and myosin filaments have been stained, ventral view; anterior up. Dashed white line indicates the anterior margin of the developing stolon head; white asterisks indicate the position of the stolon's eyes; white arrowhead pints to the position of the stolon brain; golden arrowhead points to the position of the ventrally growing pygidium immediately anterior to the stolon's head. D, Z projection of a cLSM image stack of the anterior half of a mature (released) male stolon in which tubulinergic and serotoninergic cells have been stained, dorsal view; anterior up. White asterisks indicate the position of the stolon's eyes; golden arrowhead points to the position of the stolon's brain; I-IV indicate the four main segmental nerves. Bottom-left corner shows the same Z projection but based on a reduced image stack. White arrowheads indicate the position of the circumintestinal connectives; golden line indicates the anterior margin of the stolons head. Scale bars: 50 µm.

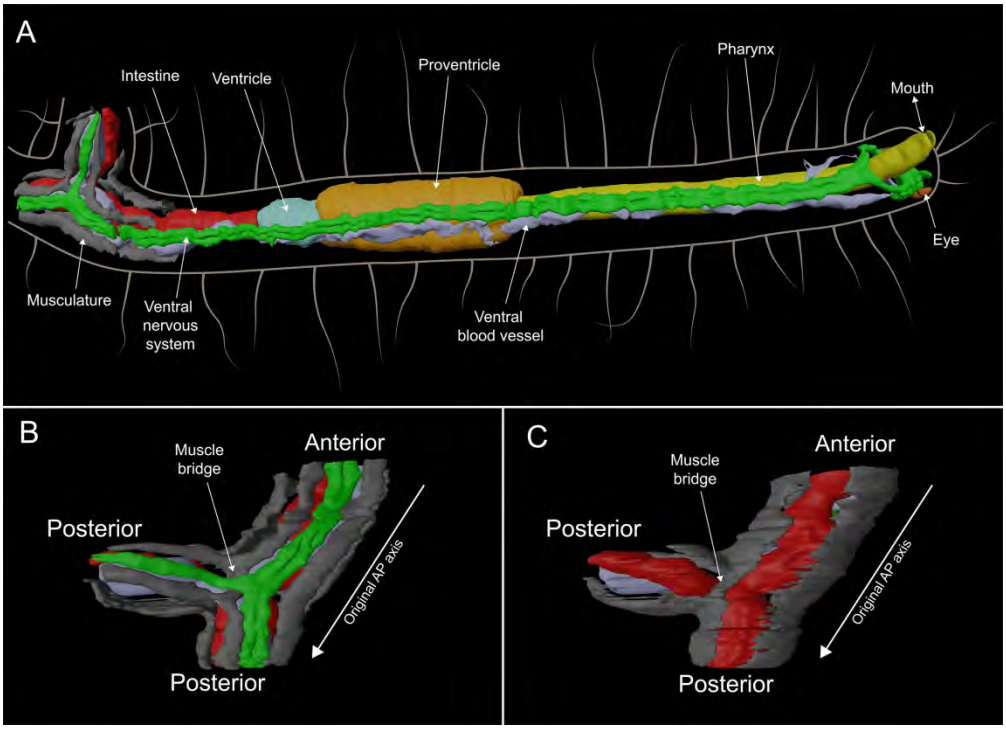

Three-dimensional reconstruction of histological sections of the anterior end of *Ramisyllis multicaudata*. A, Ventral view of the complete model from the head (right) to the first branching point (left). Grey lines indicate the body's surface, cirri, and antennae, based on a live image of a different individual. Note that musculature (dark grey) is only shown at the branching point for visualization purposes. B, Enlarged view of the branching point, ventral view. Small arrow points to the muscle bridge (dark grey) dorsally crossing over the ventral nerve cord (green). C, Enlarged view of the branching point, dorsal view. Small arrow points to the muscle bridge (dark grey) dorsally crossing over the digestive tube (red). Note that only the ventral blood vessel is represented since it is ramarkably bigger than the dorsal vessel.

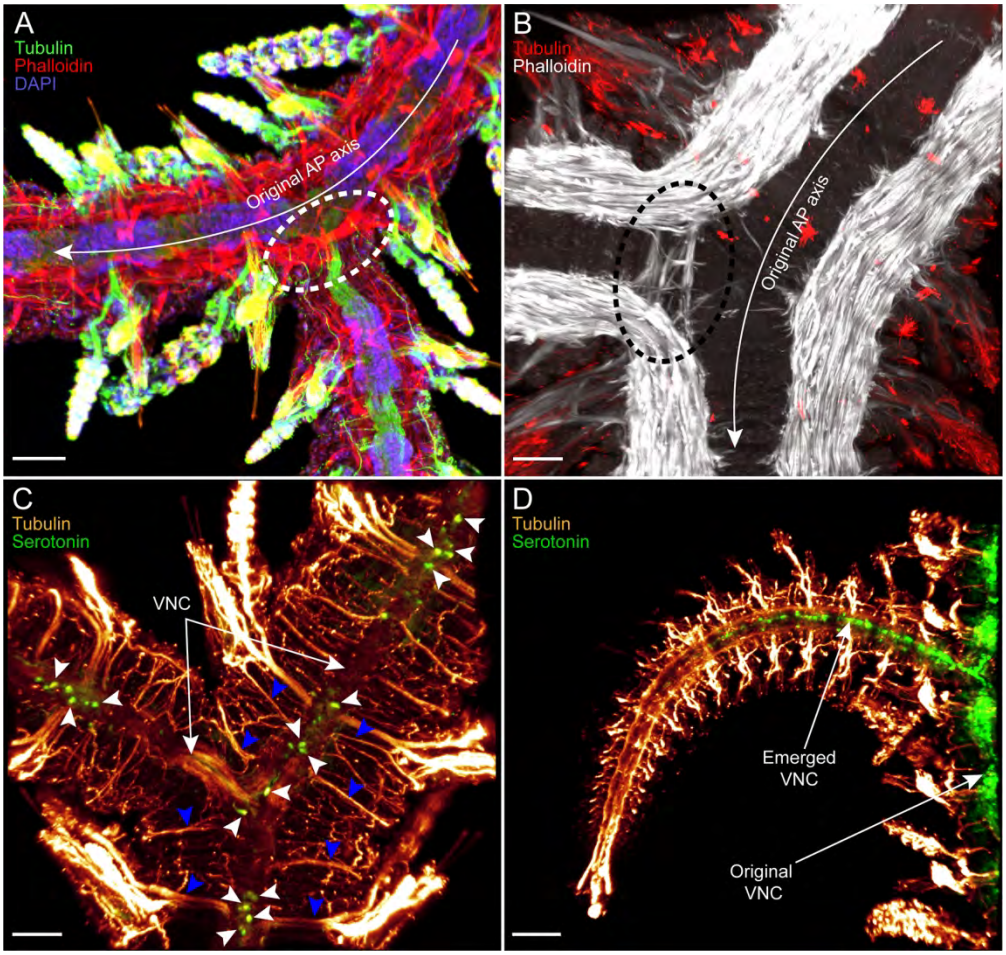

Z projection of a cLSM image stacks of immunohistochemical stainings of musculature and nervous system at the branching point. A and B, Anti-f-actin stainings confirm the presence of muscle bridges (see text) in one of the three branches coming out of a branching point. Dashed lines mark the position of the muscle bridges. C, Nervous system staining reveals the presence of the numerous serotonergic neurons characteristic of the ventral nerve cord in all three branches coming out of a branching point. Arrows point to the position of the ventral nerve cord; white arrowheads point to some of the serotonergic neurons; blue arrowheads point to the pairs of segmental neurite bundles that emerge from the ventral nerve cord but show no serotonergic neurons (note that the emerging VNC does not substitute any of the segmental neurite bundles). D, Nervous system staining in a recently emerged branch bearing a tail end, showing the presence of a complete ventral nerve cord emerging from the original one (see discussion). Scale bars: 50 µm.